



# Synthesis and characterization of dicationic and monocationic fluorine-containing DBU based ionic liquids: Experimental and quantum chemical approaches

Sara Fallah Ghasemi Gildeh, Hossein Roohi\*, Morteza Mehrdad, Kurosh Rad-Moghadam, Khatereh Ghauri

Department of Chemistry, Faculty of Science, University of Guilan, Rasht, Iran

## ARTICLE INFO

### Article history:

Received 6 May 2021

Revised 7 July 2021

Accepted 14 July 2021

Available online 18 July 2021

### Keywords:

Dicationic ionic liquids

DBU

Bis(trifluoromethanesulfonyl)imide

Trifluoromethanesulfonate

H NMR

Thermal stability

DFT

solvation energy

## ABSTRACT

In this study, the new dicationic ionic liquids (DILs) based on para-xylyl linked bis-1,8-diazobicyclo [5.4.0]undec-7-ene ( $[p-C_6H_4(CH_2DBU)_2]^{2+}$ ) dication and their corresponding monocation ionic liquids (MILs) containing the bis(trifluoromethanesulfonyl) imide  $[NTf_2]^-$  and trifluoromethanesulfonate  $[OTf]^-$  anions are synthesized. The method is based on the functionalization reaction of DBU salts using a simple procedure under microwave irradiation, followed by anion exchange. The obtained ILs are characterized by  $^1H$ -NMR,  $^{13}C$ -NMR, and FT-IR spectroscopy. The thermal decomposition of  $[p-C_6H_4(CH_2DBU)_2][NTf_2]_2$ ,  $[p-C_6H_4(CH_2DBU)_2][OTf]_2$ ,  $[C_6H_5-CH_2DBU][NTf_2]$  and  $[C_6H_5-CH_2DBU][OTf]$  ILs are measured using thermogravimetric (TGA) analyses and differential scanning calorimetry (DSC) in the temperature range from 25 to 800 °C. The thermal behavior confirmed that the DILs and MILs including  $[NTf_2]^-$  are more stable than the DILs and MILs including  $[OTf]^-$  that is in good agreement with the greater dispersion energy calculated for  $[NTf_2]^-$  based ILs. The  $[p-C_6H_4(CH_2DBU)_2][NTf_2]_2$  DIL shows good thermal stability up to 435°C which makes them suitable for thermal application. Finally, the cation-anion interactions were investigated in both DILs and MILs using DFT-M06-2X functional in conjunction with the 6-311++G(d,p) basis set. The results indicate that hydrogen bonding is stronger in the IL containing  $[OTf]^-$  anion. The calculations in the solution phase with COSMO-RS method show that the ILs including  $[OTf]^-$  anion have greater solvation energy and for the DILs are larger than those of MILs.

© 2021 Elsevier B.V. All rights reserved.

## 1. Introduction

During the last decade, ionic liquids (ILs) have been the attention of the scientific community. They because of their unique and tunable physicochemical properties have been a highly active field of research in many applications [1].

At the laboratory level, 1,8-diazobicyclo [5.4.0]undec-7-ene (DBU) is a non-nucleophilic and belongs to the family of amidine compounds that is used as catalyst in organic synthesis [2]. Reed et al. reported for the first time the remarkably strong nucleophilic behavior of DBU in the reaction with halogenated compounds [3]. DBU has excellent catalytic activity, but, the separation of DBU from the products mixture is generally difficult. The ionic liquids based on functionalized DBU as task-specific ionic liquids (TSILs) with special functions can overcome this drawback and exhibit a

similar basicity to DBU accompanied with the general features of the ILs.

The chemical reaction of the precursors as 1,8-diazobicyclo [5.4.0]undec-7-ene (DBU) with alkyl halides yields transfer of the alkyl group to the precursor ring and results in halogenides ionic liquids. Unfortunately, the range of obtained ionic liquids during this step is limited and it is not of primary concern for applications. The reaction of halogenides ionic liquids with different bulk anions opens a wide range of opportunities for obtaining new ionic liquids with special properties [4–7]. So far, many ionic liquids based on DBU include bis(trifluoromethylsulfonyl) imide, nitrate, alkyl sulphates, dicyanamide, thiocyanate, trifluoromethanesulfate, tetrafluoroborate, and hexafluorophosphate, etc. anions have been reported [8–17]. Moreover, the possibility of functionalization of DBU precursor opens up even a wider opportunity for obtaining new functionalized ionic liquid with different properties [4,6,8,18].

Recently, a new class of ionic liquids has been introduced, namely dicationic ionic liquids (DILs) [19–31]. Compared to MILs, DILs are more tunable. Because of a large number of possible

\* Corresponding author.

E-mail address: [hroohi@guilan.ac.ir](mailto:hroohi@guilan.ac.ir) (H. Roohi).

changes in cation, anion or in the side chain (linker) resulted into two head groups linked by a rigid or flexible spacer and two monoanions [19].

Compared to their monocationic counterparts, DILs usually display higher thermal stability: their thermal decomposition temperatures range from 330 °C up to 400 °C, while they can be as low as 145–185 °C for monocationic ILs. Also, the viscosity of DILs is more than that of the usual ionic liquid and the viscosity of DILs can be tuned by varying the length of the chain linking and type of anions [32–36]. DILs can be used in applications concerning lubrication at high temperatures, as an agent for the extraction of phenolic compounds from oil mixtures, as a surfactant, or as catalysts for the esterification reaction [32,36–38].

Despite the wealth of papers on based-DBU monocationic ionic liquids and their applications [8–17], there are a few experimental and computational studies on the corresponding DILs to understand the Gibbs free interaction energies, (structural, topological and electronic) properties and vibrational frequency spectra. Also, these relationships with physicochemical properties of the DILs [39].

In previous work [40], we synthesized a series of DBU-based MILs (Bn-DBU)  $[Y_{1-6}]$ , ( $Y_{1-6} = [CH_3CO_2]^-$ ,  $[C_6H_5SO_2]^-$ ,  $[HCO_3]^-$ ,  $[CF_3CO_2]^-$ ,  $[BF_4]^-$  and  $[SCN]^-$ ) and evaluated their electrochemical stability by cyclic voltammetry (CV) and theoretical computation. Also, in other research work [41], we introduced [Bn-DBU][CF<sub>3</sub>CO<sub>2</sub>] MIL as an efficient catalyst for the synthesis of 1H-pyrazolo[1,2-b]phthalazine-5,10-diones via the three-component reaction of phthalhydrazide, aromatic aldehydes, and active methylene nitriles.

In this work, the four new ( $[p-C_6H_4(CH_2DBU)_2][NTf_2]_2$  and  $[p-C_6H_4(CH_2DBU)_2][OTf]_2$ ) DILs and  $[C_6H_5-CH_2DBU][NTf_2]$  and  $([C_6H_5-CH_2DBU][OTf])$  MILs based on para-xylylene linked bis-1,8-diazobicyclo [5.4.0] undec-7-ene dication and its corresponding monocation containing the bis(trifluoromethanesulfonyl) imide  $[NTf_2]^-$  and trifluoromethanesulfonate  $[OTf]^-$  anions (Fig. 1) were synthesized and characterized by <sup>1</sup>H NMR and <sup>13</sup>C-NMR. The thermal stability of  $[p-C_6H_4(CH_2DBU)_2][NTf_2]_2$ ,  $[p-C_6H_4(CH_2DBU)_2][OTf]_2$ ,  $[C_6H_5-CH_2DBU][NTf_2]$  and  $[C_6H_5-CH_2DBU][OTf]$  ILs and their decomposition process were investigated. In addition, the energy minimum structures of the ILs were calculated at M06-2X/6-311++G(d,p) level of theory.

## 2. Experimental methods

### 2.1. Material and methods

Chemicals were purchased from Fluka, Merck, and Aldrich chemical companies and used without further purification. FT-IR spectra of the products were obtained in KBr wafers on a VERTEX 70 Bruker (Germany) instrument. <sup>1</sup>H NMR and <sup>13</sup>C NMR spectra were recorded on a Bruker (DRX-400 Avance) spectrometer at 400.22 and 100.62 MHz, respectively. The chemical shifts were measured in ppm relative to the resonance of the deuterated solvent and TMS. Thermogravimetric analyses (TGA) were performed on a DSC-TG analyzer model Q 600 TA (USA). The thermal behavior of the samples was scanned from 25 to 800 °C at the rate of 20 °C min<sup>-1</sup> under air atmosphere.

### 2.2. Synthesis of $[C_6H_5CH_2DBU][OTf]$ and $[C_6H_5CH_2DBU][NTf_2]$ MILs from $[C_6H_5CH_2DBU][Cl]$ salt

For the synthesis of  $[C_6H_5CH_2DBU]Cl$ , a mixture of DBU (0.76 g, 5 mmol) and benzyl chloride (1.01 g, 8 mmol) was heated under the microwave (360 W) for 2 periods of 1 min irradiation with a break time (of ~25 s, for temperature measurement) between them. The average temperature of the reaction mixture

during microwave irradiation was about 100 °C. After cooling at room temperature, the resulting mixture was washed with diethyl ether (3 × 5 mL) to remove the unreacted starting materials and thereby the salt  $[C_6H_5CH_2DBU]Cl$  was obtained as a brown solid in 96% yield. To derive the desirable MILs,  $[C_6H_5CH_2DBU]Cl$  (1.12 g, 4 mmol) and a slightly excess amount (0.72 g, 4.6 mmol) of  $[Li][OTf]$  or (1.32 g, 4.6 mmol) of  $[Li][NTf_2]$  were added to acetonitrile (15 mL) in a canonical flask equipped with a magnetic stirrer. The flask was sealed and stirred at room temperature for 5 h. Next, the solid phase was removed by centrifugation and the liquid phase was evaporated at 50 °C under reduced pressure to remove acetonitrile and any other volatile impurities. The viscous IL remained after evaporation of the solvent was collected and dried at 80 °C for 5 h. By this method, the MILs  $[C_6H_5CH_2DBU][OTf]$  and  $[C_6H_5CH_2DBU][NTf_2]$  were obtained in 91% and 93% yields, respectively, and have been sufficiently pure for synthetic applications, as determined by their <sup>1</sup>H NMR spectra (Scheme 1).

### 2.3. Synthesis of DILs $[p-C_6H_4(CH_2DBU)_2][OTf]_2$ and $[p-C_6H_4(CH_2DBU)_2][NTf_2]_2$ from the salt $[p-C_6H_4(CH_2DBU)_2][Br]_2$

A mixture of p-xylylene dibromide (1.32 g, 5 mmol) and DBU (1.52 g, 10 mmol) was heated under microwave (360 W) for 2 periods of 1 min irradiation with a break time (of ~25 s, for temperature measurement) between them. The average temperature of the reaction mixture during microwave irradiation was about 100 °C. The crude product was washed with diethyl ether (3 × 5 mL) to give  $[p-C_6H_4(CH_2DBU)_2]Br_2$  as a white hygroscopic solid in 97% yield. Next, to derive the desirable DILs,  $[p-C_6H_4(CH_2DBU)_2]Br_2$  (2.27 g, 4 mmol) and a slight excess amount of  $[Li][OTf]$  (1.44 g, 9.2 mmol) were added to acetonitrile (15 mL) in a canonical flask containing a magnetic stirring bar. The reaction mixture was stirred for 5 h at 50–60 °C. After this time, the solid phase was removed by centrifugation and the supernatant liquid phase was evaporated at 80 °C under reduced pressure to remove acetonitrile and any possible volatile impurities. This method gave the DIL  $[p-C_6H_4(CH_2DBU)_2][OTf]_2$  as a white amorphous solid in 95% yield, (Scheme 2). The structure of this compound has been confirmed by IR, H NMR and C NMR spectroscopy.

To achieve the synthesis of  $[p-C_6H_4(CH_2DBU)_2][NTf_2]_2$ , a mixture of  $[p-C_6H_4(CH_2DBU)_2]Br_2$  white powders (2.27 g, 4 mmol) and a slight excess amount of  $LiNTf_2$  (2.64 g, 9.2 mmol) were added to acetonitrile (15 mL) in a canonical flask containing a magnetic stirring bar. The suspension was stirred at room temperature for 5 h. After this time, the suspension was filtered off. The filtrate was washed with deionized water, evaporated under a reduced pressure at 50 °C, and dried in an oven at 80 °C for 5 h to obtain the white powder of  $[p-C_6H_4(CH_2DBU)_2][NTf_2]_2$  (Mp. 98°C) in 95% yield (Scheme 3).

The structures of these DILs have been confirmed by IR, H NMR and C NMR spectroscopy. Based on the NMR spectra, the DILs are reasonably pure for synthetic applications. The energetically optimal structures of the MILs  $[C_6H_5CH_2DBU][OTf]$  and  $[C_6H_5CH_2DBU][NTf_2]$  as well as the DILs  $[p-C_6H_4(CH_2DBU)_2][OTf]_2$  and  $[p-C_6H_4(CH_2DBU)_2][NTf_2]_2$  have been investigated at M06-2X/6-311++G(d,p) level of theory in the gas phase using DFT calculations.

## 3. Computational details

Density functional theory (DFT) was employed for predicting the geometrical structure, energetic and electronic properties and characterization of the nature of intermolecular interactions between the cation and anion of the ionic liquids. The M06-2X exchange-correlation functional with the 6-311G++(d,p) basis set was used to perform the conformational analysis and geometry

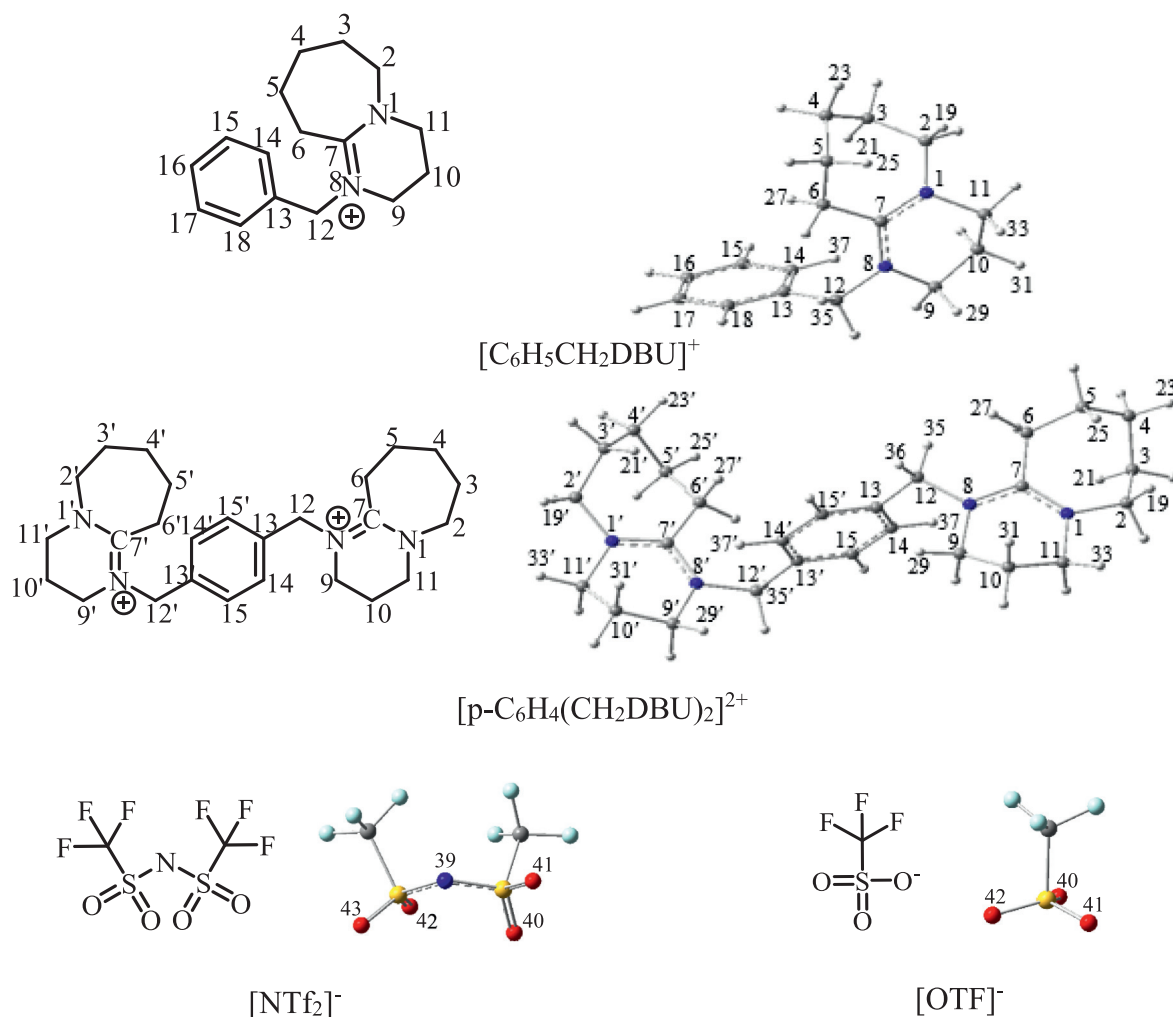
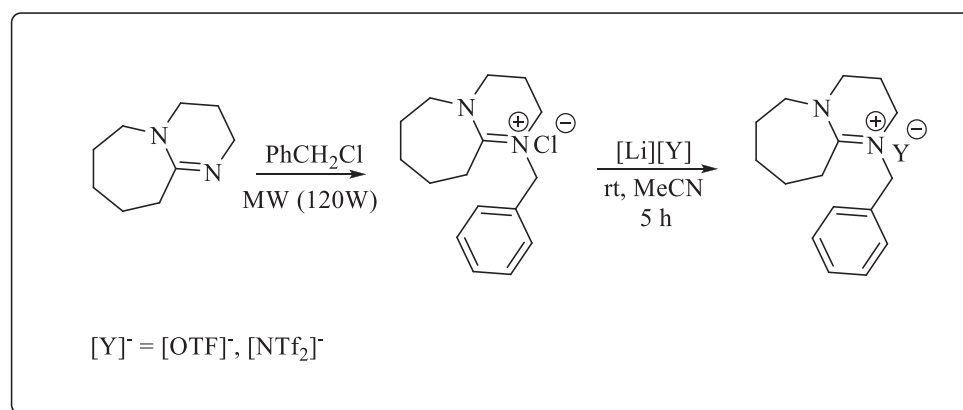


**Fig. 1.** Overview of the dication, monocation and anions optimized structures of DBU-based dicatonic and monocationic ionic liquids.



**Scheme 1.** Preparation of  $[\text{C}_6\text{H}_5\text{CH}_2\text{DBU}][\text{OTf}]$  and  $[\text{C}_6\text{H}_5\text{CH}_2\text{DBU}][\text{NTf}_2]$  MILs.

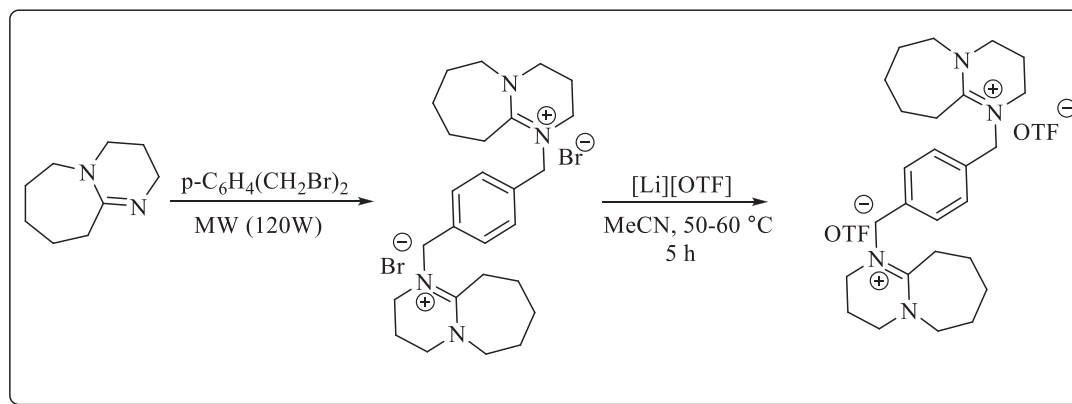
optimizations [42–44]. The interaction energies for each isolated ionic liquid were corrected with the basis set superposition error (BSSE) using the Boys Bernardi counterpoise technique (CP) [45]. To characterize the stationary points and calculation of zero-point vibrational energy (ZPVE) as well as thermochemical quantities, vibrational frequency analysis was performed at the mentioned level of theory. All the above calculations were performed by using the Gaussian program [46]. The interaction energy is defined as the difference between the energy (corrected by the ZPVE) of the sys-

tem  $E_{\text{IL}}$  and the sum of the energies of the ions ( $E_{\text{cation}} + E_{\text{anion}}$ ) by the following equation:

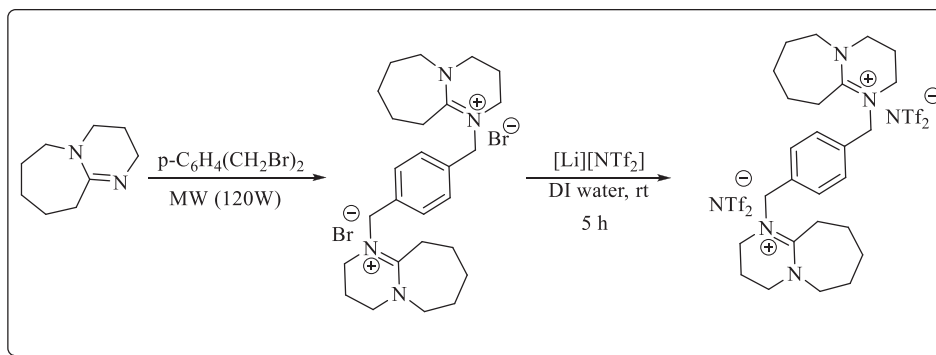
$$\Delta E (\text{kcal mol}^{-1}) = 627.51 \times [E_{\text{IL}}(au) - (E_{\text{cation}}(au) + E_{\text{anion}}(au))]$$

where  $E_{\text{IL}}$  is the electronic energy of the ionic liquid system and ( $E_{\text{cation}} + E_{\text{anion}}$ ) is the energy sum of pure cation and anion.

The electronic distribution in a molecule can be explored using the molecular electrostatic potential (MESP) topography analysis based on the electrostatic potential index,  $V(\mathbf{r})$ , [47]. The



**Scheme 2.** The reactions leading to the synthesis of  $[p\text{-C}_6\text{H}_4(\text{CH}_2\text{DBU})_2][\text{OTF}]_2$  DIL.



**Scheme 3.** The reactions leading to synthesis of  $[p\text{-C}_6\text{H}_4(\text{CH}_2\text{DBU})_2][\text{NTf}_2]_2$  DIL.

MESPs on the 0.001 au contours were calculated at the M06-2X/6-311++G(d,p) level using the Multiwfn program [48].

## 4. Results and discussion

### 4.1. Experimental results

#### 4.1.1. Spectroscopic characterization of ILS

The FT-IR and  $^1\text{H}$  NMR and  $^{13}\text{C}$  NMR spectra of the synthesized MILs and DILs were given as supplementary information in Figs. S1, S2 and S3, respectively. The  $[\text{C}_6\text{H}_5\text{CH}_2\text{DBU}][\text{OTF}]$ ,  $[\text{C}_6\text{H}_5\text{CH}_2\text{DBU}][\text{NTf}_2]$ ,  $[p\text{-C}_6\text{H}_4(\text{CH}_2\text{DBU})_2][\text{OTF}]_2$  and  $[p\text{-C}_6\text{H}_4(\text{CH}_2\text{DBU})_2][\text{NTf}_2]_2$  ILS were characterized by  $^1\text{H}$  NMR,  $^{13}\text{C}$  NMR and FT-IR as follows:

*The selected data of  $[\text{C}_6\text{H}_5\text{CH}_2\text{DBU}][\text{OTF}]$ :* Pale yellow oil;  $^1\text{H}$  NMR (DMSO- $d_6$ , 500 MHz),  $\delta_{\text{H}}$  ppm: 7.42 (2H, t,  $J$  7.6 Hz, Ar-H), 7.34 (1H, t,  $J$  7.2 Hz, Ar-H), 7.29 (2H, d,  $J$  7.6 Hz, Ar-H), 4.85 (2H, s,  $\text{CH}_2$ ), 3.67 (2H, s,  $\text{CH}_2$ ), 3.55 (2H, t,  $J$  5.4 Hz,  $\text{CH}_2$ ), 3.48 (2H, t,  $J$  5.2 Hz,  $\text{CH}_2$ ), 2.88-2.86 (2H, m,  $\text{CH}_2$ ), 2.05-2.00 (2H, m,  $\text{CH}_2$ ), 1.65-1.62 (4H, m, 2 $\text{CH}_2$ ), 1.50 (2H, br s,  $\text{CH}_2$ );  $^{13}\text{C}$  NMR (DMSO- $d_6$ )  $\delta$  ppm: 166.7, 135.5 (2C), 128.9, 127.7, 126.9, 71.4, 55.8, 54.2, 47.2, 27.7, 25.3, 22.3, 19.4; FT-IR (KBr,  $\text{cm}^{-1}$ ): 2938, 2867, 1623, 1528, 1453, 1328.

*The selected data of  $[\text{C}_6\text{H}_5\text{CH}_2\text{DBU}][\text{NTf}_2]$ :* Pale yellow oil;  $^1\text{H}$  NMR (DMSO- $d_6$ , 500 MHz),  $\delta_{\text{H}}$  ppm: 7.41 (2H, t,  $J$  7.6 Hz, Ar-H), 7.34 (1H, t,  $J$  6.7 Hz, Ar-H), 7.29 (2H, d,  $J$  7.6 Hz, Ar-H), 4.85 (2H, s,  $\text{CH}_2$ ), 3.68 (2H, s,  $\text{CH}_2$ ), 3.55 (2H, t,  $J$  5.7 Hz,  $\text{CH}_2$ ), 3.48 (2H, t,  $J$  5.7 Hz,  $\text{CH}_2$ ), 2.89-2.87 (2H, m,  $\text{CH}_2$ ), 2.05-2.00 (2H, m,  $\text{CH}_2$ ), 1.65-1.61 (4H, m, 2 $\text{CH}_2$ ), 1.51 (2H, br s,  $\text{CH}_2$ );  $^{13}\text{C}$  NMR (DMSO- $d_6$ )  $\delta$  ppm: 166.7, 135.5 (2C), 128.9, 127.8, 126.6, 55.8, 54.2, 48.6, 47.2, 27.7 (2C), 25.3, 22.3, 19.4; FT-IR (KBr,  $\text{cm}^{-1}$ ): 2937, 2867, 1624, 1528, 1453.

*The selected data of  $[p\text{-C}_6\text{H}_4(\text{CH}_2\text{DBU})_2][\text{OTF}]_2$ :* White solid paste;  $^1\text{H}$  NMR (DMSO- $d_6$ , 500 MHz),  $\delta_{\text{H}}$  ppm: 7.33 (2H, s, Ar-H), 4.87 (2H, s,  $\text{CH}_2$ ), 3.68 (2H, s,  $\text{CH}_2$ ), 3.56 (2H, t,  $J$  5.8 Hz,  $\text{CH}_2$ ), 3.48 (2H, t,  $J$  5.3 Hz,  $\text{CH}_2$ ), 2.89-2.86 (2H, m,  $\text{CH}_2$ ), 2.05-2.00 (2H, m,  $\text{CH}_2$ ), 1.66 (4H, br s, 2 $\text{CH}_2$ ), 1.50 (2H, br s,  $\text{CH}_2$ );  $^{13}\text{C}$  NMR (DMSO- $d_6$ )  $\delta$  ppm: 166.7, 162.3, 135.2, 127.2, 55.4, 54.2, 48.7, 47.2, 27.7 (2C), 25.3, 22.3, 19.4; FT-IR (KBr,  $\text{cm}^{-1}$ ): 2939, 2872, 1659, 1619, 1527, 1443, 1327.

*The selected data of  $[p\text{-C}_6\text{H}_4(\text{CH}_2\text{DBU})_2][\text{NTf}_2]_2$ :* White powder;  $^1\text{H}$  NMR (DMSO- $d_6$ , 500 MHz),  $\delta_{\text{H}}$  ppm: 7.32 (2H, s, Ar-H), 4.86 (2H, s,  $\text{CH}_2$ ), 3.68 (2H, s,  $\text{CH}_2$ ), 3.55 (2H, t,  $J$  5.7 Hz,  $\text{CH}_2$ ), 3.46 (2H, t,  $J$  5.4 Hz,  $\text{CH}_2$ ), 2.87-2.85 (2H, m,  $\text{CH}_2$ ), 2.05-2.00 (2H, m,  $\text{CH}_2$ ), 1.66 (4H, br s, 2 $\text{CH}_2$ ), 1.50 (2H, br s,  $\text{CH}_2$ );  $^{13}\text{C}$  NMR (DMSO- $d_6$ )  $\delta$  ppm: 166.7, 135.2, 127.1, 120.8, 55.4, 54.2, 48.7, 47.2, 27.7 (2C), 25.3, 22.3, 19.4; FT-IR (KBr,  $\text{cm}^{-1}$ ): 2939, 2861, 1631, 1533, 1445, 1334.

The chemical shifts of the  $\text{CH}_2$  group between DBU and phenyl rings were used for the characterization of the MILs and DILs. The chemical shifts of the  $\text{CH}_2$  group is 3.67, 4.86, 3.68 and 4.86. As can be seen, the chemical shift of the  $\text{CH}_2$  group of the ILS for the  $[\text{OTF}]^-$  anion is smaller than  $[\text{NTf}_2]^-$  ones, indicating that the strength of the interaction is further affected by the variation of the anions type rather than the cations type.

#### 4.1.2. Thermogravimetric analysis

Thermal stability as an important property of ILS depends on the type of anion and cation [49]. The thermal stability of both dicationic ionic liquids and the corresponding monocationic ionic liquids ( $[p\text{-C}_6\text{H}_4(\text{CH}_2\text{DBU})_2][\text{OTF}]_2$ ,  $[p\text{-C}_6\text{H}_4(\text{CH}_2\text{DBU})_2][\text{NTf}_2]_2$ ,  $[\text{C}_6\text{H}_5\text{CH}_2\text{DBU}][\text{OTF}]$  and  $[\text{C}_6\text{H}_5\text{CH}_2\text{DBU}][\text{NTf}_2]$ ) were evaluated by TGA and DSC that their spectra were shown in Fig. 2. The decomposition temperature ( $T_d$ ) of the new ionic liquids involves two stages within the temperature range of 400–545 °C. The TGA

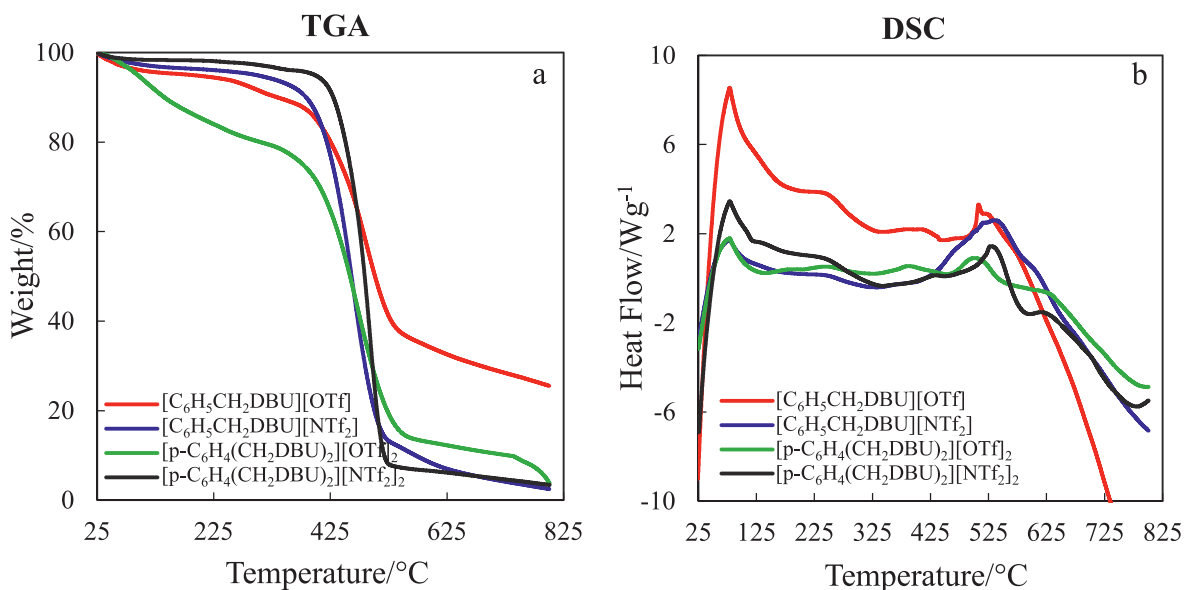


Fig. 2. (a) TGA and (b) DSC curves for  $[p\text{-C}_6\text{H}_4(\text{CH}_2\text{DBU})_2][\text{OTf}]_2$  DIL,  $[p\text{-C}_6\text{H}_4(\text{CH}_2\text{DBU})_2][\text{NTf}_2]_2$  DIL,  $[\text{C}_6\text{H}_5\text{CH}_2\text{DBU}][\text{OTf}]$  MIL and  $[\text{C}_6\text{H}_5\text{CH}_2\text{DBU}][\text{NTf}_2]$  MIL.

curve of the ILs shows that the first stage from weight-loss to the main decomposition stage can be attributed to the evaporation of adsorbed water by the samples exposed to humidity. The first stage of weight loss of mono and dicationic ionic liquids containing the  $[\text{OTf}]^-$  anion occurs over a wider temperature range and shows that the weight loss in these ILs is greater than ionic liquids containing the  $[\text{NTf}_2]^-$  anion. The initial weight-loss in the DSC curve of the ionic liquids represents an endothermic process in the range of 90–95 °C, which is related to the evaporation of adsorbed water molecules by the above samples. Main decomposition temperature ( $T_d$ ) of the ILs is initiated at 400, 420, 410 and 450 °C for  $[\text{C}_6\text{H}_5\text{CH}_2\text{DBU}][\text{OTf}]$ ,  $[\text{C}_6\text{H}_5\text{CH}_2\text{DBU}][\text{NTf}_2]$ ,  $[p\text{-C}_6\text{H}_4(\text{CH}_2\text{DBU})_2][\text{OTf}]_2$  and  $[p\text{-C}_6\text{H}_4(\text{CH}_2\text{DBU})_2][\text{NTf}_2]_2$  ILs, respectively, that indicating  $T_d$  is highly dependent on the nature of the constructive anions of the ionic liquids. Certainly, many forces such as hydrogen bonds, van der Waals forces and ion-ion interaction affect the thermal stability of the ionic liquids. The type of anion and its orientation relative to the cation affect the decomposition temperature of the ILs.

As can be seen, ILs containing the  $[\text{NTf}_2]^-$  anion are more stable than the others. DSC curve of the four  $[\text{C}_6\text{H}_5\text{CH}_2\text{DBU}][\text{OTf}]$ ,  $[\text{C}_6\text{H}_5\text{CH}_2\text{DBU}][\text{NTf}_2]$ ,  $[p\text{-C}_6\text{H}_4(\text{CH}_2\text{DBU})_2][\text{OTf}]_2$  and  $[p\text{-C}_6\text{H}_4(\text{CH}_2\text{DBU})_2][\text{NTf}_2]_2$  ionic liquids indicate two peaks that the first is in the range of 90–95 °C and the second is in the range of 545–550 °C. As can be seen, the intensity of the peaks in the range of 90–95 °C for  $[\text{C}_6\text{H}_5\text{CH}_2\text{DBU}][\text{OTf}]$  ionic liquid is much higher than other ionic liquids. The second peak can be related to the thermal decomposition of the ionic liquids.

## 4.2. Quantum mechanic results

### 4.2.1. Electrostatic potential (ESP) maps

The ESP map is a very useful descriptor in understanding electrophilic and nucleophilic attacks in chemical reactions. It can be used to recognize regions of local negative and positive potentials in a molecule and to explain the intermolecular interactions between polar species. In this paper, the interaction between cation and anion were studied. The possible interaction sites around  $[p\text{-C}_6\text{H}_4(\text{CH}_2\text{DBU})_2]^{2+}$  dications and  $[\text{C}_6\text{H}_5\text{-CH}_2\text{DBU}]^+$  monocation that  $[\text{OTf}]^-$  and  $[\text{NTf}_2]^-$  anions are approaching can be characterized from electrostatic potential ESP maps. These maps display the variably charged regions of a molecule.

Fig. 3 displays the ESP maps of the free anions and cations of  $[p\text{-C}_6\text{H}_4(\text{CH}_2\text{DBU})_2][\text{OTf}]_2$ ,  $[p\text{-C}_6\text{H}_4(\text{CH}_2\text{DBU})_2][\text{NTf}_2]_2$ ,  $[\text{C}_6\text{H}_5\text{-CH}_2\text{DBU}][\text{OTf}]$  and  $[\text{C}_6\text{H}_5\text{-CH}_2\text{DBU}][\text{NTf}_2]$  ILs assessed at M06-2X/6-311++G(d,p) level of theory, where the red-colored surfaces represent the negative electrostatic potential and the blue-colored surfaces signify the positive one. As can be observed in Fig. 3, all regions around  $[\text{C}_6\text{H}_5\text{-CH}_2\text{DBU}]^+$  and  $[p\text{-C}_6\text{H}_4(\text{CH}_2\text{DBU})_2]^{2+}$  cations have positive electrostatic potential. Because of darker blue-colored surface, the positive charge distributions were mostly located on N1, C7, N8 atoms (surface map value = 0.1402, 0.1267 and 0.1321) and C-H bonds of  $[\text{C}_6\text{H}_5\text{-CH}_2\text{DBU}]^+$  cation as well as on N1 (N1'), N8 (N8'), C7 (C7') atoms (surface map value = 0.2043 (0.1892), 0.1880 (0.1959) and 0.2081 (0.1954)) and C-H (C'-H') bonds of  $[p\text{-C}_6\text{H}_4(\text{CH}_2\text{DBU})_2]^{2+}$  dications. A negative charge concentration was seen over the oxygen atoms of  $[\text{OTf}]^-$  and  $[\text{NTf}_2]^-$  anions, respectively, as indicated by the red color. According to ESP maps, the main interactions can be occurred between the O atoms of  $[\text{OTf}]^-$  and  $[\text{NTf}_2]^-$  anions and positive regions of the cations (N1 (N1'), N8 (N8'), C7 (C7') atoms and C-H (C'-H') bonds). So, the hydrogen bonds can be formed between the O atoms of  $[\text{OTf}]^-$  and  $[\text{NTf}_2]^-$  anions and C-H (C'-H') bonds of the cations.

The value of ESP minimum ( $V_{\text{min}}$ ) in a non-covalent binding interaction is a useful parameter showing the shift of electron density from one atom to another.  $V_{\text{min}}$  in the ESP topography provides a quantitative interpretation of the basic strength and position of the lone pair. Magnitude of the sum of  $V_{\text{min}}$  values for O atoms of anions involved in interaction with the dication and monocation in the  $[p\text{-C}_6\text{H}_4(\text{CH}_2\text{DBU})_2][\text{OTf}]_2$ ,  $[p\text{-C}_6\text{H}_4(\text{CH}_2\text{DBU})_2][\text{NTf}_2]_2$ ,  $[\text{C}_6\text{H}_5\text{-CH}_2\text{DBU}][\text{OTf}]$  and  $[\text{C}_6\text{H}_5\text{-CH}_2\text{DBU}][\text{NTf}_2]$  ILs is -134.7 (-118.5), -108.2 (-99.5), -130.5 and -111.6 kcal mol<sup>-1</sup>, respectively. Its value for O atoms of isolated anions  $[\text{OTf}]^-$  and  $[\text{NTf}_2]^-$  is -364.7 and -339.1 kcal mol<sup>-1</sup>. Thus, it is estimated that the strength of the interaction is different in the DILs and MILs formed by  $[\text{OTf}]^-$  and  $[\text{NTf}_2]^-$  anions. The change in sum of  $V_{\text{min}}$  of O atoms involved in interaction with cations for  $[p\text{-C}_6\text{H}_4(\text{CH}_2\text{DBU})_2][\text{OTf}]_2$ ,  $[p\text{-C}_6\text{H}_4(\text{CH}_2\text{DBU})_2][\text{NTf}_2]_2$ ,  $[\text{C}_6\text{H}_5\text{-CH}_2\text{DBU}][\text{OTf}]$  and  $[\text{C}_6\text{H}_5\text{-CH}_2\text{DBU}][\text{NTf}_2]$  ILs are 476.1 (230.0 and 246.1 for two anion), 470.6 (231.0 and 239.7 for two anion), 234.2 and 227.6 kcal mol<sup>-1</sup>, respectively,



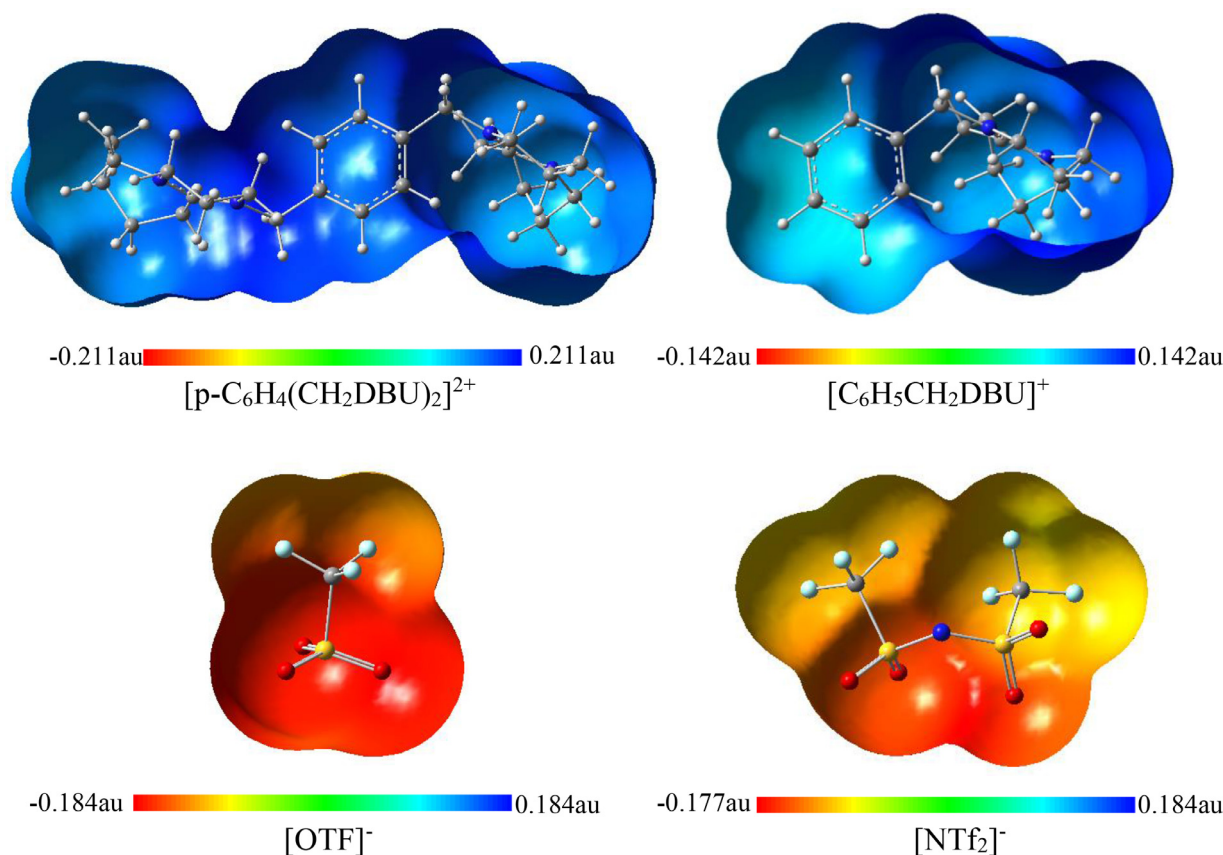


**Fig. 3.** The optimized structures and electrostatic potentials calculated at the M06-2X/6311++G(d,p) level of theory and mapped on to the 0.001 electron density isosurface for free  $[p\text{-C}_6\text{H}_4(\text{CH}_2\text{DBU})_2]^{2+}$  dication,  $[\text{C}_6\text{H}_5\text{CH}_2\text{DBU}]^+$  monocation,  $[\text{OTF}]^-$  and  $[\text{NTf}_2]^-$  anions in the gas phase.

**Table 1**

Change in zero-point energy ( $\Delta\text{ZPVE}$ ), basis set superposition error (BSSE), Electronic interaction energy ( $\Delta\text{E}$ ), corrected electronic interaction energy ( $\Delta\text{E}_c$ ) deformation energy ( $E_{\text{def}}$ ) dispersion energy ( $E_{\text{disp}}$ ) (kcal mol<sup>-1</sup>) of ILs calculated at M06-2X/6311++G(d,p) level of theory.

Structure	$\Delta\text{ZPVE}$	BSSE	$\Delta\text{E}$	$\Delta\text{E}_c$	$E_{\text{def}}$	$E_{\text{disp}}$
$[p\text{-C}_6\text{H}_4(\text{CH}_2\text{DBU})_2][\text{OTF}]_2$	3.19	7.46	-218.82	-214.08	4.89	-5.91
$[p\text{-C}_6\text{H}_4(\text{CH}_2\text{DBU})_2][\text{NTf}_2]_2$	3.08	11.13	-206.51	-199.76	6.18	-7.45
$[\text{C}_6\text{H}_5\text{CH}_2\text{DBU}][\text{OTF}]$	1.47	3.33	-90.27	-88.29	2.44	-2.82
$[\text{C}_6\text{H}_5\text{CH}_2\text{DBU}][\text{NTf}_2]$	1.47	5.39	-85.27	-82.21	2.28	-3.81

$$\Delta\text{E} = E_{\text{elec}}(\text{DIL}) - (E_{\text{elec}}(\text{Dication}) + 2E_{\text{elec}}(\text{Anion})).$$

$$\Delta\text{E}_c = \Delta\text{E} + \text{BSSE} + \Delta\text{ZPVE} + E_{\text{Dispersion}}.$$

$$E_{\text{def}} = E_{\text{dicat}}(\text{DIL}) + E_{\text{ani}}(\text{DIL}) + E_{\text{ani}}(\text{DIL}) - (E_{\text{dicat}}(\text{free}) + 2E_{\text{ani}}(\text{free})).$$

showing that the shift of electron density in the  $[\text{OTF}]^-$  anion is more than  $[\text{NTf}_2]^-$  anion when anions interact with cations in the DILs and MILs. The most stable structures of the DILs and MILs obtained from the interaction between cations ( $[p\text{-C}_6\text{H}_4(\text{CH}_2\text{DBU})_2]^{2+}$  and  $[\text{C}_6\text{H}_5(\text{CH}_2\text{DBU})]$ ) and anions ( $[\text{OTF}]^-$  and  $[\text{NTf}_2]^-$ ) are shown in Fig. 4. This figure shows that  $[\text{OTF}]^-$  and  $[\text{NTf}_2]^-$  anions locate above and nearly perpendicular to seven-membered rings of cations in  $[p\text{-C}_6\text{H}_4-(\text{CH}_2\text{DBU})_2][\text{OTF}]_2$ ,  $[p\text{-C}_6\text{H}_4-(\text{CH}_2\text{DBU})_2][\text{NTf}_2]_2$ ,  $[\text{C}_6\text{H}_5-\text{CH}_2\text{DBU}][\text{OTF}]$  and  $[\text{C}_6\text{H}_5-\text{CH}_2\text{DBU}][\text{NTf}_2]$  ILs.

#### 4.2.2. Interaction energies

The physicochemical properties of ILs are always related to the intermolecular interactions between anion and cation. The ions type and their possible configurations can have many effects on the interaction energy and physicochemical properties of the ILs [50–58]. The interaction energy ( $\Delta\text{E}$ ) of  $[p\text{-C}_6\text{H}_4-(\text{CH}_2\text{DBU})_2][\text{OTF}]_2$ ,  $[p\text{-C}_6\text{H}_4-(\text{CH}_2\text{DBU})_2][\text{NTf}_2]_2$ ,  $[\text{C}_6\text{H}_5-\text{CH}_2\text{DBU}][\text{OTF}]$  and  $[\text{C}_6\text{H}_5-\text{CH}_2\text{DBU}][\text{NTf}_2]$  ILs corrected by

the BSSE and ZPVE terms in the gas phase are reported in Table 1. Since the interactions between the anions ( $[\text{OTF}]^-$  and  $[\text{NTf}_2]^-$ ) and cations ( $[p\text{-C}_6\text{H}_4(\text{CH}_2\text{DBU})_2]^{2+}$  and  $[\text{C}_6\text{H}_5(\text{CH}_2\text{DBU})]$ ) of the DILs and MILs are influenced by van der Waals interactions, thus interaction energies were corrected by the inclusion of empirical dispersion at GD3-M06-2X/6-311++G(d,p) level of theory.

As can be seen in Table 1, electronic interaction energies ( $\Delta\text{E}_c$ ) corrected by dispersion, BSSE and ZPVE for  $[p\text{-C}_6\text{H}_4-(\text{CH}_2\text{DBU})_2][\text{OTF}]_2$  and  $[p\text{-C}_6\text{H}_4-(\text{CH}_2\text{DBU})_2][\text{NTf}_2]_2$  DILs are -214.1 and -199.8 kcal mol<sup>-1</sup> and those of  $[\text{C}_6\text{H}_5-\text{CH}_2\text{DBU}][\text{OTF}]$  and  $[\text{C}_6\text{H}_5-\text{CH}_2\text{DBU}][\text{NTf}_2]$  MILs are -88.3 and -82.2 kcal mol<sup>-1</sup> at M06-2X/6-311++G(d,p) level of theory. Based on the  $\Delta\text{E}_c$ , the following order can be obtained for strength of the cation-anion interactions in the studied ILs:  $[p\text{-C}_6\text{H}_4-(\text{CH}_2\text{DBU})_2][\text{OTF}]_2 > [p\text{-C}_6\text{H}_4-(\text{CH}_2\text{DBU})_2][\text{NTf}_2]_2 > [\text{C}_6\text{H}_5-\text{CH}_2\text{DBU}][\text{OTF}] > [\text{C}_6\text{H}_5-\text{CH}_2\text{DBU}][\text{NTf}_2]$ .

Comparison between the interaction energies of the  $[p\text{-C}_6\text{H}_4(\text{CH}_2\text{DBU})_2]$ -based DILs and  $[\text{C}_6\text{H}_5-\text{CH}_2\text{DBU}]$  based MILs shows that the magnitude of interaction energy for the DILs is

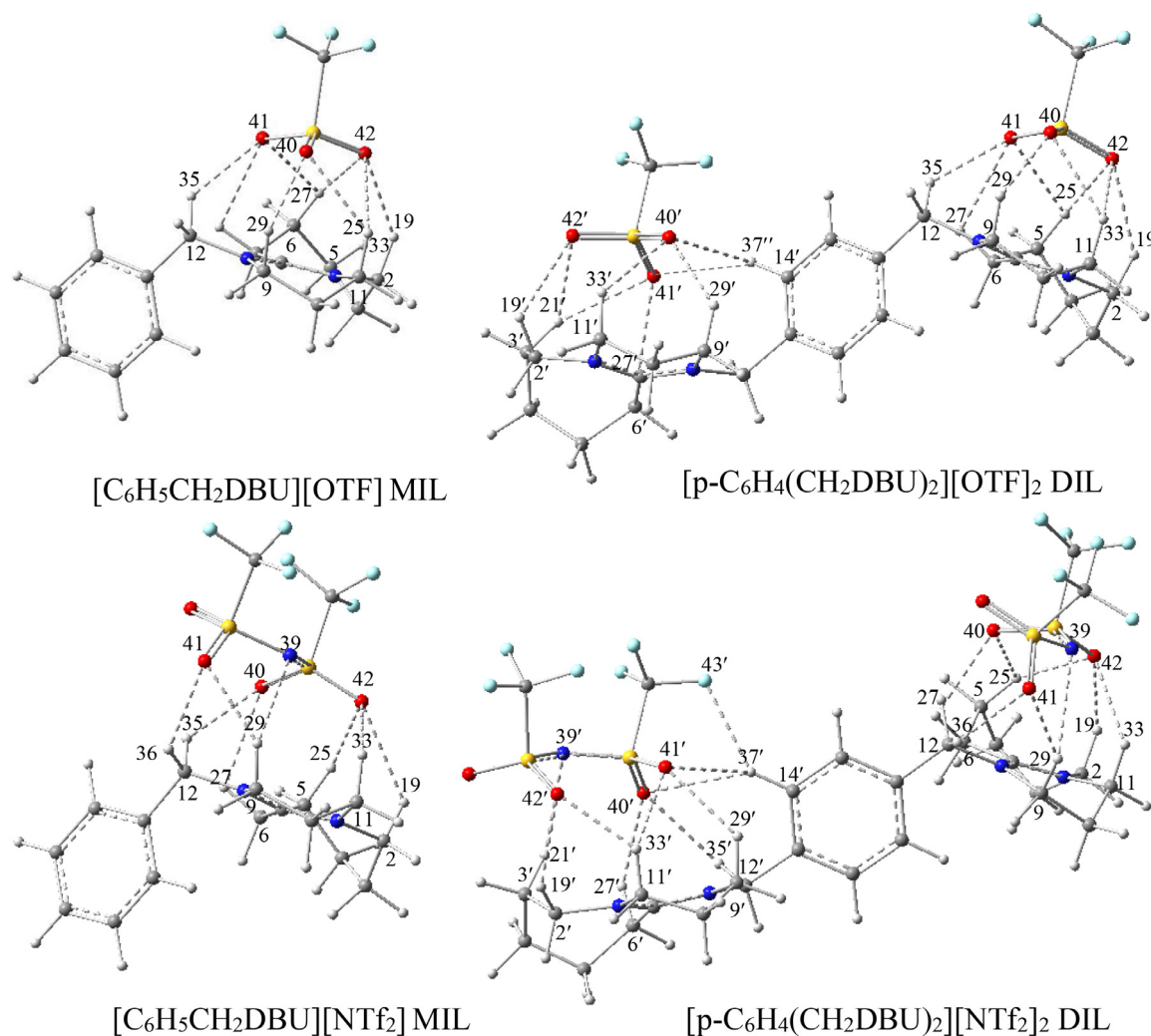


**Fig. 4.** The optimized structures at the M06-2X/6311++G(d,p) level of theory for  $[\text{C}_6\text{H}_4(\text{CH}_2\text{DBU})_2][\text{OTF}]_2$ ,  $[\text{p-C}_6\text{H}_4(\text{CH}_2\text{DBU})_2][\text{NTf}_2]_2$ ,  $[\text{C}_6\text{H}_5\text{CH}_2\text{DBU}][\text{OTF}]$  and  $[\text{C}_6\text{H}_5\text{CH}_2\text{DBU}][\text{NTf}_2]$  ILs in gas phase.

greater than the MILs and is much greater than twice the values obtained for the MILs at M06-2X/6-311++G(d,p) level of theory. The strong electrostatic attractions between the dication  $[\text{p-C}_6\text{H}_4(\text{CH}_2\text{DBU})_2]^{2+}$  and the anions may be responsible for the higher melting point and thermal stability of the DILs.

Owing to the structures of the cations and anions change upon ionic liquids formation, deformation energies ( $E_{\text{def}}$ ) of  $[\text{p-C}_6\text{H}_4(\text{CH}_2\text{DBU})_2][\text{OTF}]_2$ ,  $[\text{p-C}_6\text{H}_4(\text{CH}_2\text{DBU})_2][\text{NTf}_2]_2$ ,  $[\text{C}_6\text{H}_5\text{CH}_2\text{DBU}][\text{OTF}]$  and  $[\text{C}_6\text{H}_5\text{CH}_2\text{DBU}][\text{NTf}_2]$  ILs are calculated and given in Table 1.

The deformation energy ( $E_{\text{def}}$ ) in the DILs is calculated by equation:  $E_{\text{def}} = E_{\text{dicat(DIL)}} + E_{\text{ani(DIL)}} + E_{\text{ani'(DIL)}} - (E_{\text{dicat(free)}} + 2E_{\text{ani(free)}})$ , where the  $E_{\text{dicat(DIL)}}$  and  $E_{\text{ani(DIL)}}$  are, respectively, energy of dication and anion in the structure of optimized DIL in absence of anion and dication, and  $E_{\text{dicat,anion(free)}}$  is the energy of free optimized ions. As can be seen, the  $E_{\text{def}}$  for  $[\text{p-C}_6\text{H}_4(\text{CH}_2\text{DBU})_2][\text{OTF}]_2$  and  $[\text{p-C}_6\text{H}_4(\text{CH}_2\text{DBU})_2][\text{NTf}_2]_2$  DILs (4.9 and 6.2 kcal mol<sup>-1</sup>) are more than  $[\text{C}_6\text{H}_5\text{CH}_2\text{DBU}][\text{OTF}]$  and  $[\text{C}_6\text{H}_5\text{CH}_2\text{DBU}][\text{NTf}_2]$  MILs (2.4 and 2.3 kcal mol<sup>-1</sup>).

#### 4.2.3. Interaction Gibbs free energy and solvation energy in water

Gibbs free energy of solvation and the Gibbs free interaction energy of  $[\text{p-C}_6\text{H}_4(\text{CH}_2\text{DBU})_2][\text{OTF}]_2$ ,  $[\text{p-C}_6\text{H}_4(\text{CH}_2\text{DBU})_2][\text{NTf}_2]_2$ ,  $[\text{C}_6\text{H}_5\text{CH}_2\text{DBU}][\text{OTF}]$  and  $[\text{C}_6\text{H}_5\text{CH}_2\text{DBU}][\text{NTf}_2]$  ILs in solvent media were calculated in the water media using COSMO-RS

method at M06-2X/6-311++G(d,p) level of theory using optimized structures obtained in the gas phase. Besides, the Gibbs free interaction energies were calculated in the gas phase.

The non-electrostatic ( $\Delta G_{\text{nonelec}}^\circ$ ) and electrostatic ( $\Delta G_{\text{elec}}^\circ$ ) contributions to the Gibbs free energy of solvation ( $\Delta G_{\text{solv}}^\circ$ ), change in Gibbs free energy of solvation upon ion pair formation ( $\Delta \Delta G_{\text{solv}}^\circ$ ), interaction Gibbs free energy of the ILs in the gas phase ( $\Delta G_{\text{g}}^\circ$ ) and interaction Gibbs free energy of the ILs in water solution ( $\Delta G_{\text{solv}}^\circ$ ) are listed in Table 2.

These results reveal that the non-electrostatic contribution to the  $\Delta G_{\text{solv}}^\circ$  for the ILs in water is positive and the non-electrostatic contributions to  $\Delta G_{\text{solv}}^\circ$  is more positive for the ILs including  $[\text{NTf}_2]^-$  anion. The electrostatic contribution to  $\Delta G_{\text{solv}}^\circ$  is mainly responsible for the changes of relative energies. The order of  $\Delta G_{\text{solv}}^\circ$  values in water is as:  $[\text{p-C}_6\text{H}_4(\text{CH}_2\text{DBU})_2][\text{OTF}]_2 > [\text{p-C}_6\text{H}_4(\text{CH}_2\text{DBU})_2][\text{NTf}_2]_2 > [\text{C}_6\text{H}_5\text{CH}_2\text{DBU}][\text{OTF}] > [\text{C}_6\text{H}_5\text{CH}_2\text{DBU}][\text{NTf}_2]$ . The value of  $\Delta G_{\text{solv}}^\circ$  is a measure of the strength of the interaction between solute and solvent. Therefore, it is expected that  $\Delta G_{\text{solv}}^\circ$  be greater for the DILs and MILs having  $[\text{OTF}]^-$  anion.

The calculated dipole moment values of the ILs in both gas and water phases are 19.11 and 25.25 Debye in  $[\text{p-C}_6\text{H}_4(\text{CH}_2\text{DBU})_2][\text{OTF}]_2$ , 20.36 and 26.91 Debye in  $[\text{p-C}_6\text{H}_4(\text{CH}_2\text{DBU})_2][\text{NTf}_2]_2$ , 10.27 and 12.83 Debye in  $[\text{C}_6\text{H}_5\text{CH}_2\text{DBU}][\text{OTF}]$  and 11.37 and 14.37 Debye in  $[\text{C}_6\text{H}_5\text{CH}_2\text{DBU}][\text{NTf}_2]$ .

**Table 2**

The solvation energies ( $\Delta E_{\text{solv}} = E_{\text{elec}}(\text{solvent}) - E_{\text{elec}}(\text{gas})$ ), the electrostatic  $\Delta G_{\text{elc}}^{\circ}$ , and non-electrostatic,  $\Delta G_{\text{nonelc}}^{\circ}$ , contributions to the Gibbs free energy of solvation,  $\Delta G_{\text{solv}}^{\circ}$ , change in Gibbs free energy of solvation,  $\Delta\Delta G_{\text{solv}}^{\circ}$  of the studied ILs at M06-2X/6311++G(d,p) level using COSMO-RS method in water and also interaction Gibbs free energy of the ILs in the gas phase and water solution, ( $\Delta G_{\text{g}}^{\circ}$  and  $\Delta G_{\text{sol}}^{\circ}$ ) calculated at M06-2X/6-311++G(d,p) level of theory. All energies are in kcal mol<sup>-1</sup>.

IL	$\Delta E_{\text{solv}}$	$\Delta G_{\text{elc}}^{\circ}$	$\Delta G_{\text{nonelc}}^{\circ}$	$\Delta G_{\text{solv}}^{\circ}$	$\Delta\Delta G_{\text{solv}}^{\circ}$	$\Delta G_{\text{g}}^{\circ}$	$\Delta G_{\text{sol}}^{\circ}$
[p-C <sub>6</sub> H <sub>4</sub> (CH <sub>2</sub> DBU) <sub>2</sub> ][OTF] <sub>2</sub>	-37.51	-46.07	29.25	-16.82	200.47	-183.45	17.02
[p-C <sub>6</sub> H <sub>4</sub> (CH <sub>2</sub> DBU) <sub>2</sub> ][NTf <sub>2</sub> ] <sub>2</sub>	-38.35	-46.85	37.41	-9.44	185.95	-168.35	17.60
[C <sub>6</sub> H <sub>5</sub> CH <sub>2</sub> DBU][OTF]	-20.90	-24.60	17.12	-7.48	82.88	-73.68	9.20
[C <sub>6</sub> H <sub>5</sub> CH <sub>2</sub> DBU][NTf <sub>2</sub> ]	-20.88	-24.38	21.29	-3.09	76.32	-66.75	9.57

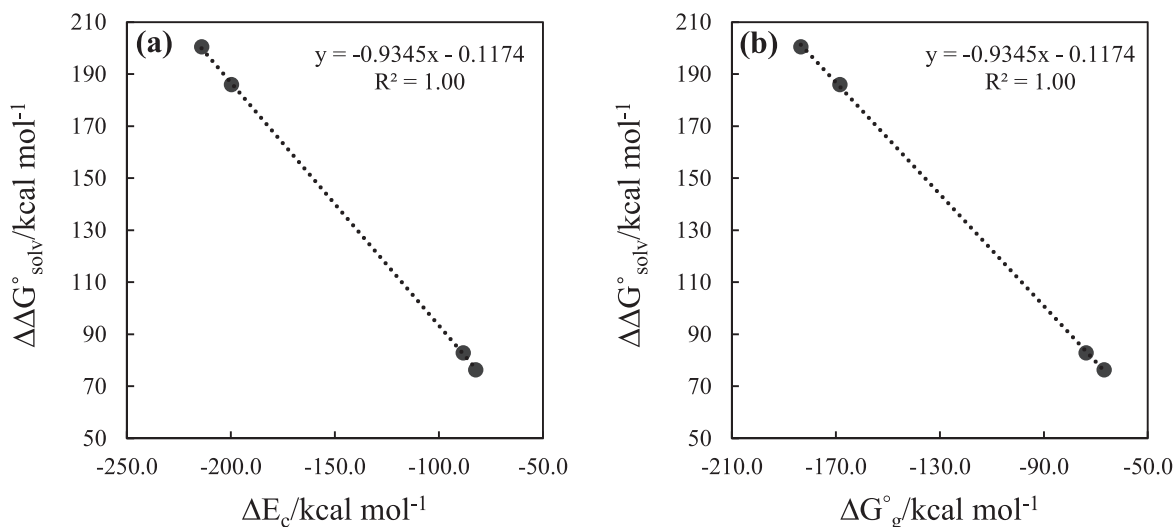


**Fig. 5.** (a) The correlation between  $\Delta\Delta G_{\text{solv}}^{\circ}$  and  $\Delta E_{\text{c}}$ , (b) The relationship between  $\Delta\Delta G_{\text{solv}}^{\circ}$  and  $\Delta G_{\text{g}}^{\circ}$  of [p-C<sub>6</sub>H<sub>4</sub>(CH<sub>2</sub>DBU)<sub>2</sub>][OTF]<sub>2</sub>, [p-C<sub>6</sub>H<sub>4</sub>(CH<sub>2</sub>DBU)<sub>2</sub>][NTf<sub>2</sub>]<sub>2</sub>, [C<sub>6</sub>H<sub>5</sub>CH<sub>2</sub>DBU][OTF] and [C<sub>6</sub>H<sub>5</sub>CH<sub>2</sub>DBU][NTf<sub>2</sub>] ILs in gas and water phases at M06-2X/6-311++G(d,p) level of theory.

[C<sub>6</sub>H<sub>5</sub>-CH<sub>2</sub>DBU][NTf<sub>2</sub>] at M06-2X/6-311++G(d,p) level of theory. The order of magnitude of the dipole moment in both phases is [p-C<sub>6</sub>H<sub>4</sub>(CH<sub>2</sub>DBU)<sub>2</sub>][NTf<sub>2</sub>]<sub>2</sub> > [p-C<sub>6</sub>H<sub>4</sub>(CH<sub>2</sub>DBU)<sub>2</sub>][OTF]<sub>2</sub> > [C<sub>6</sub>H<sub>5</sub>-CH<sub>2</sub>DBU][NTf<sub>2</sub>] > [C<sub>6</sub>H<sub>5</sub>-CH<sub>2</sub>DBU][OTF] and the dipole moment of the DILs is more than those of MILs.

As can be seen in Table 2, the values of  $\Delta\Delta G_{\text{solv}}^{\circ}$  for (cation + anion → ionic liquid) process in water are positive and increases as  $\Delta E_{\text{c}}$  of the ILs increases. Consequently, there is a correlation between  $\Delta\Delta G_{\text{solv}}^{\circ}$  and  $\Delta E_{\text{c}}$  in water (Fig. 5 (a)). The relationship between  $\Delta G_{\text{g}}^{\circ}$  ( $\Delta G_{\text{c}}$ ) and  $\Delta\Delta G_{\text{solv}}^{\circ}$  is depicted in Fig. 5(b). It is obvious from Fig. 5(b) that an increase in the absolute value of  $\Delta G_{\text{g}}^{\circ}$  is accompanied by an increase in  $\Delta\Delta G_{\text{solv}}^{\circ}$ . It is predicted that the nonspecific interactions between water and ions are notably more effective than with the ILs. In order to analyze the consequence of these results, we have also calculated the Gibbs free interaction energy of the DILs and MILs in water ( $\Delta G_{\text{sol}}^{\circ}$ ). The  $\Delta G_{\text{sol}}^{\circ}$  of the ILs in water was calculated according to the relation of  $\Delta G_{\text{sol}}^{\circ} = \Delta\Delta G_{\text{solv}}^{\circ} + \Delta G_{\text{g}}^{\circ}$ , where the  $\Delta\Delta G_{\text{solv}}^{\circ} = \Delta G_{\text{solv,IL}}^{\circ} - \sum \Delta G_{\text{solv,Ions}}^{\circ}$ . The results show that the Gibbs free interaction energy of the ILs drastically diminishes with the polarity of solvent: for example, from -183.45 kcal mol<sup>-1</sup> for [p-C<sub>6</sub>H<sub>4</sub>(CH<sub>2</sub>DBU)<sub>2</sub>][OTF]<sub>2</sub> in the gas phase to 17.02 kcal mol<sup>-1</sup> in water. From  $\Delta G_{\text{sol}}^{\circ}$  values given in Table 2, it is found that all  $\Delta G_{\text{sol}}^{\circ}$  values are positive, indicating that the degree of association of ions decreases on going from gas phase to liquid solution phase. In fact, the ILs are scarcely associated in water. Based on the equation given above, the value of  $\Delta G_{\text{sol}}^{\circ}$  depends on both  $\Delta\Delta G_{\text{solv}}^{\circ}$  and  $\Delta G_{\text{g}}^{\circ}$ . In fact, since the absolute value of  $\Delta G_{\text{g}}^{\circ}$  is negative and smaller than  $\Delta\Delta G_{\text{solv}}^{\circ}$ ,  $\Delta G_{\text{sol}}^{\circ}$  values for the ILs become positive. Therefore, the results show that the formation of the ILs in the solution phase of water is not a spontaneous process. It should be

also noted that the  $\Delta G_{\text{sol}}^{\circ}$  value of the ILs decreases on going from DILs to MILs. Therefore, as expected, ionic association of the ILs decreases in water.

The solvation energies of [p-C<sub>6</sub>H<sub>4</sub>-(CH<sub>2</sub>DBU)<sub>2</sub>][OTF]<sub>2</sub>, [p-C<sub>6</sub>H<sub>4</sub>-(CH<sub>2</sub>DBU)<sub>2</sub>][NTf<sub>2</sub>]<sub>2</sub>, [C<sub>6</sub>H<sub>5</sub>-CH<sub>2</sub>DBU][OTF] and [C<sub>6</sub>H<sub>5</sub>-CH<sub>2</sub>DBU][NTf<sub>2</sub>] ILs calculated in water media according to equation  $\Delta E_{\text{solv}} = E_{\text{elec}}(\text{solvent}) - E_{\text{elec}}(\text{gas})$  are listed in Table 2. As can be seen,  $\Delta E_{\text{solv}}$  for the ILs in water is negative, showing that the solvation process of ILs is energetically favorable. The  $\Delta E_{\text{solv}}$  values range between -20.88 kcal mol<sup>-1</sup> for [C<sub>6</sub>H<sub>5</sub>-CH<sub>2</sub>DBU][NTf<sub>2</sub>] MIL and -38.35 kcal mol<sup>-1</sup> for [p-C<sub>6</sub>H<sub>4</sub>-(CH<sub>2</sub>DBU)<sub>2</sub>][NTf<sub>2</sub>]<sub>2</sub> DIL in water. As can be seen, the solvation energies in water for the DILs are larger than those calculated in the MILs and the ILs including [NTf<sub>2</sub>]<sup>-</sup> anion have greater solvation energy. The relationship between  $\Delta E_{\text{solv}}$  and  $\Delta E_{\text{c}}$  is depicted in Fig. 6. It is obvious from Fig. 6 that an increase in the value of  $\Delta E_{\text{c}}$  is accompanied by an increase in  $\Delta E_{\text{solv}}$ .

The macroscopic properties such as melting point, critical temperature, enthalpy of vaporization and electrical conductivity can be mainly characterized by the strength of intermolecular interactions between cations and anions of the ILs [59–61]. Researchers in recent years reported the relationships between the interaction energy of ILs and their macroscopic parameters [62–65]. The results revealed that the increase in the interaction energy is accompanied by an increase in the melting points, critical-point temperature and enthalpy of vaporization of the ILs. Accordingly, it can be predicted that the melting point, critical-point temperature and enthalpy of vaporization of studied ILs decreases in the following order: [p-C<sub>6</sub>H<sub>4</sub>(CH<sub>2</sub>DBU)<sub>2</sub>][OTF]<sub>2</sub> > [p-C<sub>6</sub>H<sub>4</sub>(CH<sub>2</sub>DBU)<sub>2</sub>][NTf<sub>2</sub>]<sub>2</sub> > [C<sub>6</sub>H<sub>5</sub>-CH<sub>2</sub>DBU][OTF] > [C<sub>6</sub>H<sub>5</sub>-CH<sub>2</sub>DBU][NTf<sub>2</sub>]. From the comparison of the interaction energies of the ILs, it can be suggested



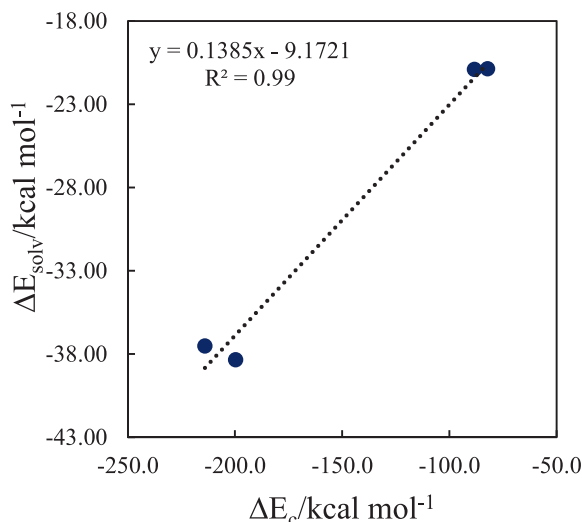


**Fig. 6.** The relationship between  $\Delta E_{\text{solv}}$  and  $\Delta E_c$  of  $[\text{C}_6\text{H}_4(\text{CH}_2\text{DBU})_2][\text{OTf}]_2$ ,  $[\text{p-C}_6\text{H}_4(\text{CH}_2\text{DBU})_2][\text{NTf}_2]_2$ ,  $[\text{C}_6\text{H}_5\text{CH}_2\text{DBU}][\text{OTf}]$  and  $[\text{C}_6\text{H}_5\text{CH}_2\text{DBU}][\text{NTf}_2]$  ILs in gas and water phases at M06-2X/6-311++G(d,p) level of theory.

that the melting points, critical-point temperature and enthalpy of vaporization of  $[\text{p-C}_6\text{H}_4(\text{CH}_2\text{DBU})_2][\text{OTf}]_2$  and  $[\text{p-C}_6\text{H}_4(\text{CH}_2\text{DBU})_2][\text{NTf}_2]_2$  DILs is greater than  $[\text{C}_6\text{H}_5\text{-CH}_2\text{DBU}][\text{OTf}]$  and  $[\text{C}_6\text{H}_5\text{-CH}_2\text{DBU}][\text{NTf}_2]$  MILs.

Also, it is predicted that the electrical conductivity of ILs decreases as the interaction energy increases. The ionic association leads to a reduction of the number of ions in the solution phase that is responsible for the reduction of the electrical conductivity of the solution. Moreover, the electrical conductivity of ILs can be affected by the relative basicity of the anions and their ability to form hydrogen bond interactions. Bernard *et al.* [66] and Panic *et al.* [67] discovered a linear correlation between the dispersion component of the binding energy (DCBE) and transport properties such as conductivity and viscosity of mentioned ILs. The greater the DCBE, the smaller is conductivity and the greater is viscosity. Therefore, dispersion interactions have a more significant effect on the transport properties of ILs. The calculated dispersion energy component of binding energy for  $[\text{C}_6\text{H}_4(\text{CH}_2\text{DBU})_2][\text{OTf}]_2$ ,  $[\text{p-C}_6\text{H}_4(\text{CH}_2\text{DBU})_2][\text{NTf}_2]_2$ ,  $[\text{C}_6\text{H}_5\text{CH}_2\text{DBU}][\text{OTf}]$  and  $[\text{C}_6\text{H}_5\text{CH}_2\text{DBU}][\text{NTf}_2]$  ILs are  $-5.91$ ,  $-7.45$ ,  $-2.82$  and  $-3.81$  kcal mol<sup>-1</sup>, respectively. Based on correlation found between DCBE and transport properties, it can be concluded that viscosity of  $\text{NTf}_2^-$  based ILs is greater than  $\text{OTf}^-$  based ones, because of greater size of  $\text{NTf}_2^-$  anion. In addition, there is a correlation between thermal stability and dispersion energy; the greater is dispersion energy, the greater is thermal stability.

#### 4.2.4. Geometrical structures

In this section, the structural parameters of the most stable configuration of the DILs and MILs based on DBU ( $[\text{p-C}_6\text{H}_4(\text{CH}_2\text{DBU})_2][\text{OTf}]_2$  DIL,  $[\text{p-C}_6\text{H}_4(\text{CH}_2\text{DBU})_2][\text{NTf}_2]_2$  DIL,  $[\text{C}_6\text{H}_5\text{CH}_2\text{DBU}][\text{OTf}]$  MIL and  $[\text{C}_6\text{H}_5\text{CH}_2\text{DBU}][\text{NTf}_2]$  MIL) are studied, as are shown in Fig. 4. The structure and size of anions as well as their possible arrangements around the cations have many effects on the structure of the MILs and DILs. In the studied MILs and DILs, anions lie above the DBU rings and through heteroatoms interact with the C–H bonds of the dication and monocation.

The optimization structural parameters show that the length of the N8–C12 bond between  $\text{CH}_2$  group and DBU ring in  $[\text{C}_6\text{H}_5\text{CH}_2\text{DBU}]^{2+}$  decreases upon MIL formation. In  $[\text{p-C}_6\text{H}_4(\text{CH}_2\text{DBU})_2]^{2+}$  dication, N8–C12 bond length is 1.469 Å that decreases to 1.467 in  $[\text{p-C}_6\text{H}_4(\text{CH}_2\text{DBU})_2][\text{OTf}]_2$  DIL and

increases to 1.471 Å in  $[\text{p-C}_6\text{H}_4(\text{CH}_2\text{DBU})_2][\text{NTf}_2]_2$  DIL, whereas N8'–C12' bond length in the dication increases from 1.475 Å in cation to 1.483 and 1.484 Å in both  $[\text{p-C}_6\text{H}_4(\text{CH}_2\text{DBU})_2][\text{OTf}]_2$  and  $[\text{p-C}_6\text{H}_4(\text{CH}_2\text{DBU})_2][\text{NTf}_2]_2$  DILs. The C2–H19 (C2'–H19'), (C3'–H21'), C5–H25, C6–H27 (C6'–H27'), C9–H29 and C11–H33 (C11'–H33') bonds of DBU rings, the C12–H35 (C12'–H35') bond of the  $\text{CH}_2$  group and C14'–H37' bond of the phenyl group in  $[\text{p-C}_6\text{H}_4(\text{CH}_2\text{DBU})_2]^{2+}$  dication and  $[\text{C}_6\text{H}_5\text{CH}_2\text{DBU}]^+$  monocation are generally involved in interaction with three O atoms of  $[\text{OTf}]^-$  and O, F and N atoms of  $[\text{NTf}_2]^-$  anions. The average value of C–H bond lengths (<C–H>) involved in H-bonding interactions decreases in the MILs and DILs upon complex formation. This decrease for  $[\text{C}_6\text{H}_5\text{-CH}_2\text{DBU}][\text{OTf}]$ ,  $[\text{C}_6\text{H}_5\text{-CH}_2\text{DBU}][\text{NTf}_2]$ ,  $[\text{p-C}_6\text{H}_4(\text{CH}_2\text{DBU})_2][\text{OTf}]_2$  and  $[\text{p-C}_6\text{H}_4(\text{CH}_2\text{DBU})_2][\text{NTf}_2]_2$  ILs is 0.002, 0.001, 0.002 and 0.001 Å, respectively, indicating that the decrease for ILs composed of  $\text{OTf}^-$  anion is greater than  $\text{NTf}_2^-$  anion. Based on decrease in C–H bond lengths upon interaction, an improper (blue-shifting hydrogen bonding) H-bonding is formed between ions in these ILs. In the improper H-bonding C–H bond is strengthened and its bond length is shortened. The C12–H35 bond length and C12–H35 (C12'–H35') bond lengths of the  $\text{CH}_2$  group increase, respectively, with formation of the MIL and DIL including  $[\text{NTf}_2]^-$  anion, whereas this bond length decreases with formation of  $[\text{p-C}_6\text{H}_4(\text{CH}_2\text{DBU})_2][\text{OTf}]_2$  DIL and  $[\text{C}_6\text{H}_5\text{-CH}_2\text{DBU}][\text{OTf}]$  MIL.

The values of H-bonding distance, C–H...X, and angle between proton donors of cations and heteroatoms of anions as proton acceptors in  $[\text{p-C}_6\text{H}_4(\text{CH}_2\text{DBU})_2][\text{OTf}]_2$ ,  $[\text{p-C}_6\text{H}_4(\text{CH}_2\text{DBU})_2][\text{NTf}_2]_2$ ,  $[\text{C}_6\text{H}_5\text{CH}_2\text{DBU}][\text{OTf}]$  and  $[\text{C}_6\text{H}_5\text{CH}_2\text{DBU}][\text{NTf}_2]$  ILs are listed in Table 3.

As can be seen in Table 3, H-bonding distance of C9H29...O40 and C12H35...O41 in all ILs smaller than other ones. These two C–H bonds are directly connected to N8 atom of six-membered ring of cation. The average values for H-bonding distances and H-bonding angles of bonds involved in interaction for  $[\text{p-C}_6\text{H}_4(\text{CH}_2\text{DBU})_2][\text{OTf}]_2$ ,  $[\text{p-C}_6\text{H}_4(\text{CH}_2\text{DBU})_2][\text{NTf}_2]_2$ ,  $[\text{C}_6\text{H}_5\text{CH}_2\text{DBU}][\text{OTf}]$  and  $[\text{C}_6\text{H}_5\text{CH}_2\text{DBU}][\text{NTf}_2]$  ILs are (2.441 Å and 125.0°), (2.467 Å and 129.0°), (2.450 Å and 124.9°) and (2.469 Å and 128.1°), respectively, The C–H...X bond angles are bent from ideal 180° to satisfy the boundary conditions required by the co-existence of different C–H...X H-bonding. As can be seen, the H-bonding distance as well as angle for ILs containing  $[\text{OTf}]^-$  anion is lower than those of  $[\text{NTf}_2]^-$  anion which is in good agreement with the greater interaction energy obtained for ILs having  $[\text{OTf}]^-$  anion.

#### 4.2.5. Electrochemical window (ECW)

Ionic liquids are generally used as an electrolyte so it is necessary to determine the electrochemical stability of the studied ILs. The electrochemical stability of an ionic liquid is determined by the width of the Electrochemical window (ECW), the voltage range in which the ionic liquid is electrochemically inert. The ECW of ILs depends mostly on the resistance of the cation against reduction and the resistance of the anion against oxidation. For this purpose, the ECW of the ionic liquids is experimentally evaluated with cyclic voltammetry measurements. Also, the ECW of the ILs can be estimated from quantum chemical calculations using difference in energy levels of HOMO of the anion and LUMO of the cation [68,69,70,71].

The HOMO and LUMO energy levels, the potentials of cathodic ( $V_{\text{CL}}$ ) and anodic limits ( $V_{\text{AL}}$ ) and ECW values of  $[\text{p-C}_6\text{H}_4(\text{CH}_2\text{DBU})_2][\text{OTf}]_2$ ,  $[\text{p-C}_6\text{H}_4(\text{CH}_2\text{DBU})_2][\text{NTf}_2]_2$ ,  $[\text{C}_6\text{H}_5\text{CH}_2\text{DBU}][\text{OTf}]$  and  $[\text{C}_6\text{H}_5\text{CH}_2\text{DBU}][\text{NTf}_2]$  ILs are also calculated theoretically in solvent acetonitrile using COSMO-RS method at BVP86/TZVP level of theory (the experimentally ECW values of ILs is usually determined in solvent acetonitrile [72]) that are listed in Table 4. The results show that the LUMO and LUMO

**Table 3**

The values of H-bonding distance (Å) and angle (°) between C-H bonds of cations as proton donors and heteroatoms of anions as proton acceptors in studied ILs.

H-bonding	[Cation][OTF] <sub>2</sub> distance(angle)	[Cation][NTf <sub>2</sub> ] <sub>2</sub> distance(angle)	[Cation][OTF] distance(angle)	[Cation][NTf <sub>2</sub> ] distance(angle)
C2H19...O42	2.372(127.3)	2.559(119.0)	2.386(126.5)	2.579(118.1)
C5H25...O41	2.574(111.9)	2.595(108.4)	2.579(112.0)	
C5H25...O42	2.428(152.1)	2.506(146.3)	2.433(151.7)	2.489(145.8)
C6H27...O41	2.563(101.7)	2.499(106.1)	2.589(101.5)	2.478(107.8)
C9H29...O40	2.264(125.2)	2.233(141.9)	2.274(125.5)	2.250(141.4)
C9H29...N39		2.694(124.6)		2.692(124.6)
C11H33...O40	2.400(130.8)		2.452(131.0)	
C11H33...O42	2.662(118.9)	2.432(120.9)	2.626(119.4)	2.425(120.8)
C12H35...O41	2.278(131.1)		2.263(132.0)	2.369(135.7)
C12H36...O40		2.453(131.5)		2.467(130.3)
C2'H19'...O42'	2.463(109.8)	2.304(135.0)		
C3'H21'...O42'	2.499(114.4)			
C3'H21'...O41'	2.485(149.6)			
C3'H21'...N39'		2.525(138.7)		
C6'H27'...O40'		2.362(123.3)		
C6'H27'...O41'	2.403(119.8)			
C9'H29'...O40'	2.226(127.2)			
C9'H29'...O41'		2.375(128.3)		
C11'H33'...O40'	2.416(125.8)			
C11'H33'...O41'		2.494(126.7)		
C11'H33'...O42'		2.244(129.8)		
C12'H35'...O40'		2.496(121.3)		
C14'H37'...O40'	2.385(107.8)	2.639(140.0)		
C14'H37'...O41'	2.644(147.0)	2.588(139.7)		
C14'H37'...F43'		2.403(139.5)		
<sup>a</sup> Δ<C-H>	0.002	0.001	0.002	0.001
<sup>b</sup> <R <sub>H</sub> ...X>	2.441	2.467	2.451	2.469
<sup>c</sup> <C-H...X>	125.0	129.0	124.9	128.1

<sup>a</sup> The change in average value of C-H bond lengths.

<sup>b</sup> The average values of H-bonding distances.

<sup>c</sup> The average values of H-bonding angles.

**Table 4**

The HOMO and LUMO energy level of isolated dication, cation and anions, the cathodic and anodic limit potentials ( $V_{CL}$  and  $V_{AL}$ ) and electrochemical window (ECW) of [p-C<sub>6</sub>H<sub>4</sub>(CH<sub>2</sub>DBU)<sub>2</sub>][OTF]<sub>2</sub>, [p-C<sub>6</sub>H<sub>4</sub>(CH<sub>2</sub>DBU)<sub>2</sub>][NTf<sub>2</sub>]<sub>2</sub>, [C<sub>6</sub>H<sub>5</sub>CH<sub>2</sub>DBU][OTF] and [C<sub>6</sub>H<sub>5</sub>CH<sub>2</sub>DBU][NTf<sub>2</sub>] ILs are theoretically calculated by COSMO-RS method at BVP86/TZVP level of theory in acetonitrile solvent.

Ions	dication	cation	[OTF] <sup>-</sup>	[NTf <sub>2</sub> ] <sup>-</sup>
E <sub>HOMO</sub> /eV	-6.92	-6.03	-6.38	-7.02
E <sub>LUMO</sub> /eV	-2.81	-1.57	0.88	-0.48
IE/eV	6.92	6.03	6.38	7.02
EA/eV	2.81	1.57	-0.88	0.48
<b>ILs</b>	<b>[cation][OTF]<sub>2</sub></b>	<b>[cation][NTf<sub>2</sub>]<sub>2</sub></b>	<b>[cation][OTF]</b>	<b>[cation][NTf<sub>2</sub>]</b>
V <sub>AL</sub> /V	6.38	6.92	6.03	6.03
V <sub>CL</sub> /V	2.81	2.81	1.57	1.57
ECW/V	3.58	4.12	4.46	4.46

$$V_{AL} = -E_{HOMO}/e^- = V_{AL}^{CPCM} = \min(V_{AL,C}^{CPCM}, V_{AL,A}^{CPCM})$$

$$V_{CL} = -E_{LUMO}/e^- = V_{CL}^{CPCM} = \max(V_{CL,C}^{CPCM}, V_{CL,A}^{CPCM})$$

$$ECW = V_{AL} - V_{CL}$$

energy levels of the dication and monocations solely determines the resistance of [p-C<sub>6</sub>H<sub>4</sub>(CH<sub>2</sub>DBU)<sub>2</sub>][NTf<sub>2</sub>]<sub>2</sub>, [C<sub>6</sub>H<sub>5</sub>CH<sub>2</sub>DBU][OTF] and [C<sub>6</sub>H<sub>5</sub>CH<sub>2</sub>DBU][NTf<sub>2</sub>] ILs against reduction and oxidation. The cathodic stability of [p-C<sub>6</sub>H<sub>4</sub>(CH<sub>2</sub>DBU)<sub>2</sub>]<sup>2+</sup> dication (2.81 V) against reduction is more than [C<sub>6</sub>H<sub>5</sub>CH<sub>2</sub>DBU]<sup>+</sup> monocation (1.57 V) in acetonitrile solvent. Comparison of HOMO energy of the anions with HOMO energy of the cations in [p-C<sub>6</sub>H<sub>4</sub>(CH<sub>2</sub>DBU)<sub>2</sub>][NTf<sub>2</sub>]<sub>2</sub>, [C<sub>6</sub>H<sub>5</sub>CH<sub>2</sub>DBU][OTF] and [C<sub>6</sub>H<sub>5</sub>CH<sub>2</sub>DBU][NTf<sub>2</sub>] ILs shows that anodic stabilities can be characterized by the corresponding dication and monocation (6.92 and 6.03 V). In [p-C<sub>6</sub>H<sub>4</sub>(CH<sub>2</sub>DBU)<sub>2</sub>][OTF]<sub>2</sub> DIL, the cathodic stability and anodic stability are determined by [p-C<sub>6</sub>H<sub>4</sub>(CH<sub>2</sub>DBU)<sub>2</sub>]<sup>2+</sup> dication (2.81V) and [OTF]<sup>-</sup> anion (6.38V). The anodic stability of the DILs and MILs are in the following order [p-C<sub>6</sub>H<sub>4</sub>(CH<sub>2</sub>DBU)<sub>2</sub>][NTf<sub>2</sub>]<sub>2</sub> > [p-C<sub>6</sub>H<sub>4</sub>(CH<sub>2</sub>DBU)<sub>2</sub>][OTF]<sub>2</sub> > [C<sub>6</sub>H<sub>5</sub>CH<sub>2</sub>DBU][OTF] ≈ [C<sub>6</sub>H<sub>5</sub>CH<sub>2</sub>DBU][NTf<sub>2</sub>] and are in good agreement with those of calculated by Ong et al. and Özdemir et al. [73,74]. The ECW values calcu-

lated for [p-C<sub>6</sub>H<sub>4</sub>(CH<sub>2</sub>DBU)<sub>2</sub>][OTF]<sub>2</sub>, [p-C<sub>6</sub>H<sub>4</sub>(CH<sub>2</sub>DBU)<sub>2</sub>][NTf<sub>2</sub>]<sub>2</sub>, [C<sub>6</sub>H<sub>5</sub>CH<sub>2</sub>DBU][OTF] and [C<sub>6</sub>H<sub>5</sub>CH<sub>2</sub>DBU][NTf<sub>2</sub>] ILs are 3.58, 4.12, 4.46 and 4.46 V in acetonitrile solvent. The ECW values of [C<sub>6</sub>H<sub>5</sub>CH<sub>2</sub>DBU][OTF] and [C<sub>6</sub>H<sub>5</sub>CH<sub>2</sub>DBU][NTf<sub>2</sub>] MILs is the same. Inspection of ECW values reveals a correlation between V<sub>AL</sub> and ECW values. The electrochemical windows of the DIL containing [NTf<sub>2</sub>]<sup>-</sup> anion is more than [OTF]<sup>-</sup> anion. The ECW values of the MILs are more than those of corresponding DILs. Therefore, MILs are the most stable ILs while [p-C<sub>6</sub>H<sub>4</sub>(CH<sub>2</sub>DBU)<sub>2</sub>][OTF]<sub>2</sub> DIL is the least stable one among the ILs examined in this work.

## 5. Conclusions

In this work, new class of DBU-based dication ionic liquids consist of the [p-C<sub>6</sub>H<sub>4</sub>(CH<sub>2</sub>DBU)<sub>2</sub>]<sup>2+</sup> dication and [OTF]<sup>-</sup> and [NTf<sub>2</sub>]<sup>-</sup> anions and corresponding mono ionic liquids were synthesized and identified. The obtained ILs are characterized by

<sup>1</sup>H-NMR, <sup>13</sup>C-NMR, and FT-IR spectroscopy. The thermal decomposition of [p-C<sub>6</sub>H<sub>4</sub>(CH<sub>2</sub>DBU)<sub>2</sub>][NTf<sub>2</sub>]<sub>2</sub>, [p-C<sub>6</sub>H<sub>4</sub>(CH<sub>2</sub>DBU)<sub>2</sub>][OTf]<sub>2</sub>, [C<sub>6</sub>H<sub>5</sub>-CH<sub>2</sub>DBU][NTf<sub>2</sub>] and [C<sub>6</sub>H<sub>5</sub>-CH<sub>2</sub>DBU][OTf] ILs are measured using thermogravimetric (TGA) analyses and differential scanning calorimetry (DSC) in the temperature range from 25 to 800°C. The thermal behavior confirmed that the DILs and MILs including [NTf<sub>2</sub>]<sup>-</sup> are more stable than the DILs and MILs including [OTf]<sup>-</sup>. The [p-C<sub>6</sub>H<sub>4</sub>(CH<sub>2</sub>DBU)<sub>2</sub>][NTf<sub>2</sub>]<sub>2</sub> DIL shows good thermal stability up to 435°C which makes them suitable for thermal application. The structural characteristics and interactions energies of the DILs and MILs were investigated at M06-2X/6-311++G(d,p) level of theory. Among the studied DILs and MILs, ILs including [OTf]<sup>-</sup> anion have stronger hydrogen bonds than those having [NTf<sub>2</sub>]<sup>-</sup> anions and in turn have the greater interaction energy. From the calculated interaction energies (ΔG<sub>g</sub>) of the DILs and MILs it can be estimated that the thermal stability of the DILs is more than MILs with the same anion. From the corrected interaction energy (ΔE<sub>c</sub>) values, it can be predicted that the melting point and enthalpy of vaporization of the DILs increases as the ΔE<sub>c</sub> increases. It is found a direct correlation between dispersion energy and viscosity as well as thermal stability of ILs. The ECW values calculated of [C<sub>6</sub>H<sub>5</sub>CH<sub>2</sub>DBU][NTf<sub>2</sub>] and C<sub>6</sub>H<sub>5</sub>CH<sub>2</sub>DBU][OTf] MLs is more the corresponding DILs.

### Author Statement

The all authors contributed to the design and implementation of the research, to the analysis of the results and to the revising of the manuscript.

### Declaration of Competing Interest

The authors declare no competing financial interest.

### Supplementary materials

Supplementary material associated with this article can be found, in the online version, at doi:10.1016/j.molstruc.2021.131123.

### CRediT authorship contribution statement

**Sara Fallah Ghasemi Gildeh:** Software, Investigation, Formal analysis, Writing – review & editing. **Hossein Roohi:** Software, Investigation, Formal analysis, Writing – review & editing. **Morteza Mehrdad:** Software, Investigation, Formal analysis, Writing – review & editing. **Kurosh Rad-Moghadam:** Software, Investigation, Formal analysis, Writing – review & editing. **Khatereh Ghauri:** Software, Investigation, Formal analysis, Writing – review & editing.

### References

- [1] R.D. Rogers, K.R. Seddon, Ionic liquids–solvents of the future? *Science* 302 (5646) (2003).
- [2] N. Ghosh, DBU (1,8-diazabicyclo[5.4.0]undec-7-ene) - A Nucleophilic Base, *Synlett* (3) (2004) 574–575, doi:10.1055/s-2004-815436.
- [3] R. Reed, R. Reau, F. Dahan, G. Bertrand, DBU and DBN are strong nucleophiles: X-ray crystal structures of onio- and dionio-substituted phosphanes, *Angew. Chem. Int. Ed. Engl.* 32 (1993) 399, doi:10.1002/anie.199303991.
- [4] S. Mahajan, R. Sharma, R.K. Mahajan, Interactions of new 1, 8-diazabicyclo [5.4.0] undec-7-ene (DBU) based surface active ionic liquids with amitriptyline hydrochloride: Micellization and interfacial studies, *Colloids Surf. A* 424 (2013) 96–104, doi:10.1016/j.colsurfa.2013.02.032.
- [5] B. Yu, H. Zhang, Y. Zhao, S. Chen, J. Xu, L. Hao, Z. Liu, DBU-based ionic-liquid-catalyzed carbonylation of o-phenylenediamines with CO<sub>2</sub> to 2-benzimidazolones under solvent-free conditions, *ACS Catal.* 3 (2013) 2076–2082, doi:10.1021/cs400256j.
- [6] Z. Wang, Z.P. Li, Y.H. Jin, W. Liu, L.H. Jiang, Q.H. Zhang, Organic superbase derived ionic liquids based on the TFSI anion: synthesis, characterization, and electrochemical properties, *New J. Chem.* 41 (2017) 5091–5097, doi:10.1039/C7NJ00407A.
- [7] A.G. Ying, L.M. Wang, L.L. Wang, X.Z. Chen, W.D. Ye, Green and efficient Knoevenagel condensation catalysed by a DBU based ionic liquid in water, *J. Chem. Res.* 34 (2010) 30–33, doi:10.3184/030823409X12616597939085.
- [8] K.C. Lethesh, S.N. Shah, M.I. Abdul Mutalib, Synthesis, Characterization, and thermophysical properties of 1,8- diazobicyclo [5.4.0]undec-7-ene based thio-cyanate ionic liquids, *J. Chem. Eng. Data* 59 (2014) 1788–1795, doi:10.1021/je400991s.
- [9] M. K.Munshi, P.S. Biradar, S.M. Gade, V.H. Rane, A.A. Kelkar, Efficient synthesis of glycerol carbonate/glycidol using 1,8-diazabicyclo [5.4.0] undec-7-ene (DBU) based ionic liquids as catalyst, *RSC Adv.* 4 (2014) 17124–17128, doi:10.1039/C3RA47433J.
- [10] M.K. Munshi, S.M. Gade, M.V. Mane, D. Mishra, S. Pal, K. Vanka, V.H. Rane, A.A. Kelkar, 1,8-Diazabicyclo[5.4.0]undec-7-ene (DBU): a highly efficient catalyst in glycerol carbonate synthesis, *J. Mol. Catal. A Chem.* 391 (2014) 144–149, doi:10.1016/j.molcata.2014.04.016.
- [11] K.J. Jisha, D. Singh, G. Sharma, R.L. Gardas, Effect of temperature on apparent molar properties of DBU based protic ionic liquid in aqueous and ethanolic solutions, *J. Mol. Liquids* 231 (2017) 213–219, doi:10.1016/j.molliq.2017.02.006.
- [12] J. Nowicki, M. Muszyńska, S. Gryglewicz, Novel basic ionic liquids from cyclic guanidines and amidines - new catalysts for transesterification of oleochemicals, *J. Chem. Technol. Biotechnol.* 89 (1) (2014) 48–55, doi:10.1002/jctb.4114.
- [13] J. Nowicki, M. Muszynski, J-P. Mikkola, Ionic liquids derived from organosuperbases: en route to superionic liquids, *R. Soc. Chem.* 6 (2016) 9194–9208, doi:10.1039/c5ra23616a.
- [14] V. Singh1, D. Singh, R.L. Gardas, Effect of DBU (1,8-diazobicyclo[5.4.0]undec-7-ene) based protic ionic liquid on the volumetric and ultrasonic properties of ascorbic acid in aqueous solution, *Ind. Eng. Chem. Res.* 54 (7) (2015) 2237–2245, doi:10.1021/ie504938.
- [15] B. Wang, Z. Luo, E.H.M. Elageed, S. Wu, Y. Zhang, X. Wu, F. Xia, G. Zhang, G. Gao, DBU and DBU-derived ionic liquid synergistic catalysts for the conversion of carbon dioxide/carbon disulfide to 3-aryl-2-oxazolimidones/[1,3]dithiolan-2-ylidene phenylamine, *ChemCatChem.* 8 (2016) 830–838, doi:10.1002/cctc.201500928.
- [16] X. Zhu, M. Song, Y. Xu, DBU-Based Protic Ionic Liquids for CO<sub>2</sub> Capture, *ACS Sustain. Chem. Eng.* 5 (9) (2017) 8192–8198, doi:10.1021/acssuschemeng.7b01839.
- [17] D. Singh, V. Singh, N. Islam, R.L. Gardas, Elucidation of molecular interactions between DBU based protic ionic liquid and organic solvents: thermophysical and computational studies, *RSC Adv.* 6 (2016) 623–631, doi:10.1039/C5RA18843A.
- [18] L. Wu, J. Song, B. Zhang, B. Zhou, H. Zhou, H. Fan, Y. Yang, B. Han, Very efficient conversion of glucose to 5-hydroxymethylfurfural in DBU-based ionic liquids with benzenesulfonate anion, *Green Chem.* 16 (2014) 3935–3941, doi:10.1039/C4GC00311J.
- [19] J.L. Anderson, R. Ding, A. Ellern, D.W. Armstrong, Structure and properties of high stability geminal dicationic ionic liquids, *J. Am. Chem. Soc.* 127 (2005) 593–604, doi:10.1021/ja046521u.
- [20] T. Payagala, J. Huang, Z.S. Breitbach, P.S. Sharma, D.W. Armstrong, Unsymmetrical dicationic ionic liquids: manipulation of physicochemical properties using specific structural architectures, *Chem. Mater.* 19 (2007) 5848–5850, doi:10.1021/cm702325a.
- [21] H. Sun, D. Zhang, C. Liu, C. Zhang, Geometrical and electronic structures of the dication and ion pair in the geminal dicationic ionic liquid 1,3-bis [3-methylimidazolium-yl] propane bromide, *J. Mol. Struct. THEOCHEM* 900 (2009) 37–43, doi:10.1016/j.theochem.2008.12.024.
- [22] J.H. Liang, X.Q. Ren, J.T. Wang, M. Jinag, Z.J. Li, Preparation of biodiesel by transesterification from cottonseed oil using the basic dication ionic liquids as catalysts, *J. Fuel Chem. Technol.* 38 (2010) 275–280, doi:10.1016/S1872-5813(10)60033-3.
- [23] A. Chinnappan, H. Kim, Environmentally benign catalyst: synthesis, characterization, and properties of pyridinium dicationic molten salts (ionic liquids) and use of application in esterification, *Chem. Eng. J.* 187 (2012) 283–288, doi:10.1016/j.cej.2012.01.101.
- [24] A. Chinnappan, H. Kim, C. Baskar, I.T. Hwang, Hydrogen generation from the hydrolysis of sodium borohydride with new pyridinium dicationic salts containing transition metal complexes, *Int. J. Hydrog. Energy* 37 (2012) 10240–10248, doi:10.1016/j.ijhydene.2012.04.021.
- [25] D. Farmanzadeh, A. Soltanabadi, S. Yeganegi, DFT study of the geometrical and electronic structures of geminal dicationic ionic liquids 1,3-bis[3-methylimidazolium-1-yl] hexane halides, *J. Chin. Chem. Soc.* 60 (2013) 551–558, doi:10.1002/jccs.201200400.
- [26] B. Haddad, A. Paolone, D. Villemin, J-F. Lohier, M. Drai, S. Bresson, E.B.O.Abbas, Para-Xylyl bis(1-methylimidazolium bis(trifluoromethanesulfonyl)imide: synthesis, crystal structure, thermal stability, vibrational studies, *J. Mol. Liquids* 260 (2018) 391–402, doi:10.1016/j.molliq.2018.03.113.
- [27] A.N. Masri, A. Mutalib MI, J-M. Leveque, A review on dicationic ionic liquids: classification and application, *Ind. Eng. Manag.* 5 (4) (2016) 197–203, doi:10.4172/2169-0316.1000197.
- [28] S.M. Alavi, S. Yeganegi, DFT study of structures and hydrogen bonds of imidazolium based halogen-free boron containing dicationic ionic liquids, *J. Mol. Liquids* 256 (2018) 330–343, doi:10.1016/j.molliq.2018.02.066.
- [29] M. Boumediene, B. Haddad, A. Paolone, M. Drai, D. Villemin, M. Rahmouni, S. Bresson, O. Abbas, Synthesis, thermal stability, vibrational spectra and conformational studies of novel dicationic meta-xylyl linked bis-1-methylimidazolium ionic liquids, *J. Mol. Struct.* 1186 (2019) 68–79, doi:10.1016/j.molstruc.2019.03.019.



- [30] O. Goli Jolodar, K. Ghauri, M. Seddighi, F. Shirini, Y. Bayat, Preparation and characterization of ethane-1,2-diaminium trinitromethanide as a novel energetic ionic liquid, *J. Mol. Struct.* 1186 (2019) 448–457, doi:10.1016/j.molstruc.2019.03.062.
- [31] H. Roohi, S. Fallah Ghasemi Gildeh, K. Ghauri, P. Fathei, Physicochemical properties of the imidazolium-based dicationic ionic liquids (DILs) composed of ethylene  $\pi$ -spacer by changing the anions: a quantum chemical approach, *Ionics* (2019), doi:10.1007/s11581-019-03325-6.
- [32] T. Moumene, E. H. Belarbi, B. Haddad, D. Villemin, O. Abbas, B. Khelifa, S. Bresson, Vibrational spectroscopic study of ionic liquids: Comparison between monocationic and dicationic imidazolium ionic liquids, *J. Mol. Struct.* 1065 (2014) 86–92, doi:10.1016/j.molstruc.2014.02.034.
- [33] H. Sun, D. Zhang, C. Liu, C. Zhang, Geometrical and electronic structures of the dication and ion pair in the geminal dicationic ionic liquid 1,3-bis[3-methylimidazolium-yl]propane bromide, *J. Mol. Struct. THEOCHEM* (2009) 90037–90043, doi:10.1016/j.theochem.2008.12.024.
- [34] H. Shirota, T. Mandai, H. Fukazawa, T. Kato, Comparison between dicationic and monocationic ionic liquids: liquid density, thermal properties, surface tension, and shear viscosity, *J. Chem. Eng. Data* 56 (2011) 2453–2459, doi:10.1021/jc2000183.
- [35] P.K. Sahu, A. Ghosh, M. Sarkar, Understanding structure–property correlation in monocationic and dicationic ionic liquids through combined fluorescence and pulsed-field gradient (PFG) and relaxation NMR experiments, *J. Phys. Chem. B* 119 (44) (2015) 14221–14235, doi:10.1021/acs.jpcc.5b07357.
- [36] R.A. Patil, M. Talebi, C. Xu, S.S. Bhawal, D.W. Armstrong, Synthesis of thermally stable geminal dicationic ionic liquids and related ionic compounds: an examination of physicochemical properties by structural modification, *Chem. Mater.* 28 (12) (2016) 4315–4323, doi:10.1021/acs.chemmater.6b01247.
- [37] C.P. Frizzo, I.M. Gindri, C.R. Bender, A.Z. Tier, M.A. Villetti, D.C. Rodrigues, M.A. Martins, Effect on aggregation behavior of long-chain spacers of dicationic imidazolium-based ionic liquids in aqueous solution, *Colloids Surf. A Physicochem. Eng. Asp.* 468 (2015) 285–294, doi:10.1016/j.colsurfa.2014.12.029.
- [38] D. Zhao, M. Liu, J. Zhang, J. Li, P. Ren, Synthesis, characterization, and properties of imidazole dicationic ionic liquids and their application in esterification, *Chem. Eng. J.* 221 (2013) 99–104, doi:10.1016/j.cej.2013.01.077.
- [39] Y. Liu, G. Mao, H. Zhao, J. Song, H. Han, Z. Li, W. Chu, Z. Sun, DBU-Based dicationic ionic liquids promoted esterification reaction of carboxylic acid with primary chloroalkane under mild conditions, *Catal. Lett.* 47 (2017) 2764–2771, doi:10.1007/s10562-017-2184-4.
- [40] S. Fallah Ghasemi Gildeh, H. Roohi, M. Mehrdad, K. Rad-Moghadam, K. Ghauri, Experimental and theoretical probing of the physicochemical properties of ionic liquids composed of [Bn-DBU] cation and various anions, *J. Mol. Struct.* 1202 (2020) 127226–127239, doi:10.1016/j.molstruc.2019.127226.
- [41] S. Fallah-Ghasemi Gildeh, M. Mehrdad, H. Roohi, K. Ghauri, S.F-G Gildeh, K. Rad-Moghadam, Experimental and DFT mechanistic insights into one-pot synthesis of 1H-pyrazolo[1,2-b]-phthalazine-5,10-diones under catalysis of DBU-based ionic liquids, *New J. Chem.* 44 (2020) 16594–16601, doi:10.1039/D0NJ03478A.
- [42] Y. Zhao, D.G. Truhlar, The M06 suite of density functionals for main group thermochemistry, thermochemical kinetics, noncovalent interactions, excited states, and transition elements: two new functionals and systematic testing of four M06-class functionals and 12 other functionals, *Theor. Chem. Acc.* 120 (2008) 215–241, doi:10.1007/s00214-007-0310-x.
- [43] Y. Zhao, D.G. Truhlar, Density Functionals with Broad Applicability in chemistry, *Acc. Chem. Res.* 41 (2008) 157–167, doi:10.1021/ar700111a.
- [44] A.D. McLean, G.S. Chandler, Contracted Gaussian basis sets for molecular calculations. I. second row atoms, *Z = 11–18*, *J. Chem. Phys.* 72 (1980) 5639–5648, doi:10.1063/1.438980.
- [45] S.F. Boys, F. Bernardi, The calculation of small molecular interactions by the differences of separate total energies. some procedures with reduced errors, *J. Mol. Phys.* 19 (1970) 553–566, doi:10.1080/00268977000101561.
- [46] M.J. Frisch, G.W. Trucks, H.B. Schlegel, G.E. Scuseria, M.A. Robb, J.R. Cheeseman, G. Scalmani, V. Barone, B. Mennucci, G.A. Petersson, H. Nakatsuji, M. Caricato, X. Li, H.P. Hratchian, A.F. Izmaylov, J. Bloino, G. Zheng, J.L. Sonnenberg, M. Hada, M. Ehara, K. Toyota, R. Fukuda, J. Hasegawa, M. Ishida, T. Nakajima, Y. Honda, O. Kitao, H. Nakai, T. Vreven, J.A. Montgomery, J.E. Peralta Jr., F. Ogliaro, M. Bearpark, J.J. Heyd, E. Brothers, K.N. Kudin, V.N. Staroverov, R. Kobayashi, J. Normand, K. Raghavachari, A. Rendell, J.C. Burant, S.S. Iyengar, J. Tomasi, M. Cossi, N. Rega, J.M. Millam, M. Klene, J.E. Knox, J.B. Cross, V. Bakken, C. Adamo, J. Jaramillo, R. Gomperts, R.E. Stratmann, O. Yazyev, A.J. Austin, R. Cammi, C. Pomelli, J.W. Ochterski, R.L. Martin, K. Morokuma, V.G. Zakrzewski, G.A. Voth, P. Salvador, J.J. Dannenberg, S. Dapprich, A.D. Daniels, O. Farkas, J.B. Foresman, J.V. Ortiz, J. Cioslowski, D.J. Fox, *Gaussian 09, Revision A.02*, Inc., Wallingford, CT, Gaussian, 2009.
- [47] P. Politzer, D.G. Truhlar, *Chemical Applications of Atomic and Molecular Electrostatic Potentials: Reactivity, Structure, Scattering, and Energetics of Organic, Inorganic, and Biological Systems*, Springer, New York, 2013.
- [48] T. Lu, F.W. Chen, Multiwfn: a multifunctional wavefunction analyzer, *J. Comput. Chem.* 33 (2012) 580–592, doi:10.1002/jcc.22885.
- [49] B.C. Ranu, S. Banerjee, R. Janu, Ionic liquid as catalyst and solvent: the remarkable effect of a basic ionic liquid, [bmim]OH on Michael addition and alkylation of active methylene compounds, *Tetrahedron* 63 (2007) 776–782, doi:10.1016/j.tet.2006.10.077.
- [50] B. Haddad, A. Paolone, M. Draï, M. Boumediene, D. Villemin, M.R. E. Belarbi, S. Bresson, Para-xylyl linked bis-imidazolium ionic liquids: a study of the conformers of the cation and of the anion-cation hydrogen bonding, *J. Mol. Struct.* 1175 (2019) 175–184, doi:10.1016/j.molstruc.2018.07.096.
- [51] Y.S. Ding, M. Zha, J. Zhang, S.S. Wang, Synthesis, characterization and properties of geminal imidazolium ionic liquids, *Colloids Surf. A Physicochem. Eng. Asp.* 298 (2007) 201–205, doi:10.1016/j.colsurfa.2006.10.063.
- [52] Z.X. Zhang, H.Y. Zhou, L. Yang, K. Tachibana, K. Kamijima, Asymmetrical dicationic ionic liquids based on both imidazolium and aliphatic ammonium as potential electrolyte additives applied to lithium secondary batteries, *Electrochim. Acta* 53 (2008) 4833–4838, doi:10.1016/j.electacta.2008.02.008.
- [53] J.C. Chang, W.Y. Ho, I.W. Sun, Y.K. Chou, H.H. Hsieh, Synthesis and properties of new ( $\mu$ -oxo) bis [trichloroferrate (III)] dianion salts incorporated with dicationic moiety, *Polyhedron* 29 (2010) 2976–2984, doi:10.1016/j.poly.2010.08.010.
- [54] J.C. Chang, W.Y. Ho, I.W. Sun, Y.L. Tung, M.C. Tsui, Synthesis and characterization of dicationic ionic liquids that contain both hydrophilic and hydrophobic anions, *Tetrahedron Lett.* 66 (2010) 6150–6155, doi:10.1016/j.tet.2010.05.105.
- [55] J.C. Chang, W.Y. Ho, I.W. Sun, Y.K. Chou, H.H. Hsieh, Synthesis and properties of new tetrachlorocobaltate (II) and tetrachloromanganate (II) anion salts with dicationic counterions, *Polyhedron* 30 (2011) 497–507, doi:10.1016/j.poly.2010.11.009.
- [56] H. Shirota, T. Mandai, H. Fukazawa, T. Kato, Comparison between dicationic and monocationic ionic liquids: liquid density, thermal properties, surface tension, and shear viscosity, *J. Chem. Eng. Data* 56 (2011) 2453–2459, doi:10.1021/jc2000183.
- [57] Z. Zhang, L. Yang, S. Luo, M. Tian, K. Tachibana, Ionic liquids based on aliphatic tetraalkylammonium dications and TFSI anion as potential electrolytes, *J. Power Sources* 167 (2007) 217–222, doi:10.1016/j.jpowsour.
- [58] M. Boumediene, B. Haddad, A. Paolone, M. Draï, D. Villemin, M. Rahmouni, S. Bresson, O. Abbas, Synthesis, thermal stability, vibrational spectra and conformational studies of novel dicationic meta-xylyl linked bis-1-methylimidazolium ionic liquids, *J. Mol. Struct.* 1186 (2019) 68–79, doi:10.1016/j.molstruc.2019.03.019.
- [59] T. Schulz, S. Ahrens, D. Meyer, C. Allolio, A. Peritz, T. Strassner, Electronic effects of para-substitution on the melting points of TAAILs, *Chem. Asian J.* 1004 (6) (2011) 863–867, doi:10.1002/asia.201000744.
- [60] A.T. De La Hoz, U.G. Brauer, K.M. Miller, Physicochemical and thermal properties for a series of 1-alkyl-4-methyl-1, 2, 4-triazolium bis (trifluoromethylsulfonfyl) imide ionic liquids, *J. Phys. Chem. B* 118 (2014) 9944–9951, doi:10.1021/jp505592t.
- [61] L.A. Daily, K.M. Miller, Correlating structure with thermal properties for a series of 1-alkyl-4-methyl-1, 2, 4-triazolium ionic liquids, *J. Org. Chem.* 78 (2013) 4196–4201, doi:10.1021/jo400393z.
- [62] K. Dong, S. Zhang, X.Y. D. Wang, Hydrogen bonds in imidazolium ionic liquids, *J. Phys. Chem. A* 110 (2006) 9775–9782, doi:10.1021/jp054054c.
- [63] S. Ahrens, A. Peritz, T. Strassner, Tunable aryl alkyl ionic liquids (TAAILs): the next generation of ionic liquids, *Angew. Chem. Int. Ed.* 48 (2009) 7908–7910, doi:10.1002/anie.200903399.
- [64] A. Nazet, S. Sokolov, T. Sonnleitner, T. Makino, M. Kanakubo, R. Buchner, Densities, viscosities, and conductivities of the imidazolium ionic liquids [Emim][Ac], [Emim][FAP], [Bmim][BETI], [Bmim][FSI], [Hmim][TFSI], and [Omim][TFSI], *J. Chem. Eng. Data* 60 (8) (2015) 2400–2411, doi:10.1021/acs.jced.5b00285.
- [65] A. Boruñi, C. Fernandez, A. Bald, Conductance Studies of Aqueous Ionic Liquid Solutions [emim][BF<sub>4</sub>] and [bmim][BF<sub>4</sub>] at Temperatures from (283.15 to 318.15) K, *Int. J. Electrochem. Sci.* 10 (2015) 2120–2129.
- [66] U.L. Bernard, E.I. Izgorodina, D.R. MacFarlane, New insights into the relationship between ion-pair binding energy and thermodynamic and transport properties of ionic liquids, *J. Phys. Chem. C* 114 (2010) 20472–20478, doi:10.1021/jp1048875.
- [67] J. Panic, A. Tot, N. Jankovi, P. Drid, S. Gadzuric, M. Vranes, Physicochemical and structural properties of lidocaine-based ionic liquids with anti-inflammatory anions, *RSC Adv.* 10 (2020) 14089–14098, doi:10.1039/C9RA08815F.
- [68] S.P. Ong, O. Andreussi, Y. Wu, N. Marzari, G. Ceder, Electrochemical windows of room-temperature ionic liquids from molecular dynamics and density functional theory calculations, *Chem. Mater.* 23 (11) (2011) 2979–2986.
- [69] S.P. Ong, G. Ceder, Investigation of the effect of functional group substitutions on the gas-phase electron affinities and ionization energies of room-temperature ionic liquids using density functional theory, *Electrochim. Acta* 55 (2010) 3804–3811, doi:10.1016/j.electacta.2010.01.091.
- [70] W. Buijs, G.J. Witkamp, M.C. Kroon, Correlation between quantumchemically calculated LUMO energies and the electrochemical window of ionic liquids with reduction-resistant anions,
- [71] J.B. Goodenough, Y. Kim, Challenges for rechargeable Li batteries, *Chem. Mater.* 22 (2010) 587–603.
- [72] M.C. Buzzeo, C. Hardacre Prof, R.G. Compton Prof, Extended electrochemical windows made accessible by room temperature ionic liquid/organic solvent electrolyte systems, *Chem. Phys. Chem.* 7 (1) (2006) 176–180, doi:10.1002/cphc.200500361.
- [73] X-Z. Yuan, V. Alzate, Z. Xie, D.G. Ivey, E. Dy, W. Qu, Effect of water and dimethyl sulfoxide on oxygen reduction reaction in bis(trifluoromethanesulfonyl)imide-based ionic liquids, *J. Electrochem. Soc.* 161 (4) (2014) 458–466, doi:10.1149/2.010404jes.
- [74] S.P. Ong, O. Andreussi, Y. Wu, N. Marzari, G. Ceder, Electrochemical windows of room-temperature ionic liquids from molecular dynamics and density functional theory calculations, *Chem. Mater.* 23 (2011) 2979–2986, doi:10.1021/cm200679y.